

Discretizing quantum field theories for quantum simulation

Terry Farrelly^{1,2,*} and Julien Streich^{1,†}

¹*Institut für Theoretische Physik, Leibniz Universität Hannover, Germany*

²*ARC Centre for Engineered Quantum Systems, School of Mathematics and Physics, University of Queensland, Brisbane, QLD 4072, Australia*

One of the exciting possibilities offered by quantum computers is their potential to efficiently simulate quantum field theories. So far, the quantum algorithms proposed to do this rely on first simulating (continuous-time) Hamiltonian lattice quantum field theory as a stepping stone to approximate the dynamics of the quantum field. Here we suggest cutting out the middleman, by showing that local unitary circuits can be meaningful regularizations of a quantum field theory. This can be done with timestep proportional to the spatial lattice spacing, giving a strict lightcone on the lattice, making the circuit a quantum cellular automaton. First, we consider the case of interacting scalar ϕ^4 theory. We give two different quantum circuits corresponding to the free field dynamics. These are simple to solve, and by considering a discrete-time version of the interaction picture, one gets the Feynman rules for the interacting versions. In fact, one of the circuits is equivalent to the real-time path integral in the discrete-time Lagrangian formulation of lattice QFT. We also extend this to non-abelian gauge fields on the lattice, showing that the path integral expression for amplitudes has an exact decomposition in terms of a finite-depth local unitary circuit. This has implications for quantum simulations of quantum field theory, suggesting that a timestep of size proportional to the spatial lattice spacing is sufficient for convergence to the right physics. This is crucial in practice for some experiments where there is a lower bound on the possible timestep length.

I. INTRODUCTION

Calculations in quantum field theory become particularly difficult in cases where perturbative methods no longer work, usually when interactions are strong. To get around this, lattice quantum field theory was introduced [1–4] to regulate QFT while allowing classical computers to perform calculations for strongly coupled fields. The lattice method applied to quantum chromodynamics has been particularly successful in calculating particle mass ratios [5] and studying phases of gauge theories, e.g., [6, 7]. Unfortunately, dynamical simulations of lattice QFT suffer from the same problem that most classical simulations of quantum many-body systems do: the memory required grows exponentially with the system size. To remedy this, quantum algorithms for simulations of some QFTs were introduced in [8–16], and it is conceivable that these should find application in the near term on relatively small quantum computers [17–19], with pioneering experiments already being performed [20, 21]. Aside from simulating physics, there are other reasons to consider such quantum algorithms. Much like how discretizing QFT for classical simulations led to a new understanding of QFT and renormalization [22], discretizations of QFT aimed at quantum simulations may offer new insights into fundamental physics.

Previously proposed quantum algorithms for QFT in, e.g., [9, 11] approximate the continuous-time lattice Hamiltonian dynamics by a quantum circuit (via a

Suzuki-Trotter decomposition) with a timestep δt . Then by taking δt sufficiently small, one can approximate the dynamics of the lattice QFT (with a fixed spatial lattice spacing a) to the desired accuracy. Then one repeats this procedure for smaller and smaller a to extrapolate to the continuum limit. In contrast, here we argue that choosing a quantum circuit with $\delta t = a$ is sufficient to simulate the QFT. This is vital for experiments in cases where technical limitations lead to a minimal timestep, e.g., to avoid unwanted spin-motion coupling when applying Mølmer-Sørensen gates in trapped ions [23]. Furthermore, in any current experiment it is highly desirable to minimize the number of gates used to achieve the same task with fewer errors, e.g., simulating some system for a time t . In fact, the timestep scaling $\delta t \propto a$ (in units with $c = 1$) is actually the best we could hope for for any circuit with a fixed interaction range over each timestep (e.g., nearest neighbour or next-nearest neighbour). Any “better” scaling, say $\delta t \propto a^{1/2}$, would mean that the lightcone of the circuit would eventually become narrower than the physical lightcone as $a \rightarrow 0$, and the circuit would fail to simulate all of the physics.

Here we first consider quantum-circuit discretizations of interacting scalar field theory that have some appealing properties. The first is that the number of local unitary gates is proportional to the spacetime volume. The second is that there is a strict upper bound on the speed of information propagation at the discrete scale. There is more than one possible circuit with all the properties that we want, but it turns out that the circuit arising from Strang splitting of the lattice QFT unitary works quite well since it turns out to be equivalent to the discrete-time path integral expression for an amplitude. We also introduce another circuit, not arising from

*Electronic address: farreltc@tcd.ie

†Electronic address: julien-streich@gmx.de

a Suzuki-Trotter decomposition or path integral, which has the right continuum limit in the free case but suffers from a bosonic analogue of fermion doubling, which can be remedied with a slightly modified interaction. This illustrates an important point: it is possible (and may also be pragmatic) to consider circuits not arising from any conventional lattice field theory but still giving the right continuum limit. Finally, we also look at pure non-abelian gauge theory on the lattice, where we also see that the discrete-time path integral amplitude is exactly equal to a sequence of finite-depth local circuits with timestep $\delta t = a$.

These quantum-circuits are also quantum cellular automata, which are discrete spacetime quantum systems where information propagates at a bounded speed [24, 25]. This property, of strictly bounded propagation speeds, is actually impossible for a continuous-time system with a local Hamiltonian on a lattice [26]. In fact, there have been proposals for discretizing QFT via quantum cellular automata in the past, but most corresponded to free QFTs [27–31] or integrable QFTs in one space dimension [32–34]. (Another approach discretizes fermions interacting with an abelian gauge field [35, 36], but it is not clear whether the fermion doubling problem [37] could be avoided.)

This work is organized as follows. In section II, we recap the essentials of scalar field theory in the Hamiltonian formulation of lattice QFT. Then in section III, we discretize the free scalar field via two quantum circuits, given in sections III A and III D. In section III C, the free circuits are solved, giving the free particles. Note that the circuits are presented in terms of field operators on a discrete lattice, as how to discretize the field operators themselves is well understood [9, 18, 38]. In section IV, we include a ϕ^4 -type interaction. By considering a discrete-time version of the interaction picture, we then work out the Feynman rules in section IV A for the interacting models. We then calculate the one-loop correction to the mass of the field in one dimension as an example illustrating the expected logarithmic divergence. This is non-trivial for the circuit of section III D, as it has no immediate connection to lattice QFT. Finally, in section V we consider non-abelian gauge fields, and show, via a simple argument, that the path integral expression for the amplitude is exactly equal to a sequence of finite-depth local circuits with timestep $\delta t = a$.

II. HAMILTONIAN LATTICE SCALAR FIELD THEORY

Let us look at the basics of lattice QFT. For a start we will focus on the continuous-time Hamiltonian version of lattice QFT [39]. This is essentially always the formalism of choice for quantum simulations of QFT. Nevertheless, in section III, we will argue that the discrete-time Lagrangian formalism is sometimes more suitable for quantum simulations. Of course, in the continuum limit, all

formalisms will agree.

Here we will look at Hamiltonian lattice QFT in the case of ϕ^4 theory, a theory of a scalar field with self interactions. The details of the continuum theory are recapped in appendix A. Here we regulate the continuum theory by considering a discrete spatial lattice with coordinates given by vectors of integers $\mathbf{n} \in \mathbb{Z}^d$ and spatial lattice spacing a . At each lattice site there are continuous degrees of freedom with dimensionless on-site operators $X_{\mathbf{n}}$ and $P_{\mathbf{n}}$, which satisfy

$$[X_{\mathbf{m}}, P_{\mathbf{n}}] = i\delta_{\mathbf{m},\mathbf{n}} \quad (1)$$

and $[X_{\mathbf{m}}, X_{\mathbf{n}}] = [P_{\mathbf{m}}, P_{\mathbf{n}}] = 0$. In terms of these we define the discrete quantum field operators:

$$\begin{aligned} X_{\mathbf{n}} &= a^{(d-1)/2}\phi_{\mathbf{n}} \\ P_{\mathbf{n}} &= a^{(d+1)/2}\pi_{\mathbf{n}}, \end{aligned} \quad (2)$$

which satisfy the canonical commutation relations

$$[\phi_{\mathbf{m}}, \pi_{\mathbf{n}}] = \frac{i}{a^d}\delta_{\mathbf{m},\mathbf{n}} \quad (3)$$

and $[\phi_{\mathbf{m}}, \phi_{\mathbf{n}}] = [\pi_{\mathbf{m}}, \pi_{\mathbf{n}}] = 0$ for all \mathbf{m} and \mathbf{n} . The factor of $1/a^d$ in equation (3) ensures that we recover the continuum commutation relations as the lattice spacing goes to zero, and the factors in equation (2) ensure the field operators have the correct dimensions.

The continuous-time dynamics is described by a Hamiltonian, and one possible choice of lattice Hamiltonian for ϕ^4 theory is given by

$$H_{\text{latt}} = a^d \sum_{\mathbf{n} \in \mathbb{Z}} \left[\frac{1}{2}\pi_{\mathbf{n}}^2 + \frac{1}{2}(\nabla_a \phi_{\mathbf{n}})^2 + \frac{m^2}{2}\phi_{\mathbf{n}}^2 + \frac{\lambda}{4!}\phi_{\mathbf{n}}^4 \right], \quad (4)$$

where the discrete gradient is chosen such that

$$(\nabla_a \phi_{\mathbf{n}})^2 = \sum_{\mathbf{e} \in \mathcal{N}} \left(\frac{\phi_{\mathbf{n}+\mathbf{e}} - \phi_{\mathbf{n}}}{a} \right)^2, \quad (5)$$

where \mathcal{N} is the set of lattice basis vectors, i.e., $\mathcal{N} = \{(1, 0, \dots, 0), \dots, (0, \dots, 0, 1)\}$. There are other choices for the discrete gradient, which may be more accurate in practice, but here we have chosen the simplest.

It will be useful later for us if we rewrite the Hamiltonian as

$$H_{\text{latt}} = H_P + H_X, \quad (6)$$

where, writing $\mu = ma$ and $\Lambda = \lambda a^{3-d}$, we have

$$\begin{aligned} H_X &= \frac{1}{a} \sum_{\mathbf{n} \in \mathbb{Z}} \left[(d + \mu^2/2)X_{\mathbf{n}}^2 - \sum_{\mathbf{e} \in \mathcal{N}} X_{\mathbf{n}+\mathbf{e}}X_{\mathbf{n}} + \frac{\Lambda}{4!}X_{\mathbf{n}}^4 \right] \\ H_P &= \frac{1}{2a} \sum_{\mathbf{n} \in \mathbb{Z}} P_{\mathbf{n}}^2. \end{aligned} \quad (7)$$

III. QUANTUM CIRCUITS FOR SCALAR FIELD THEORY

In contrast to Hamiltonian lattice QFT, our circuit discretization involves evolution in discrete time via a unitary operator. Then there is not necessarily a natural way to associate a Hamiltonian to the system, except in the continuum limit. It is enough for us that the dynamics coincides with the continuum QFT dynamics when we take a continuum limit.

The operators and Hilbert space are the same as those we saw in section II arising in lattice quantum field theory. To simplify our notation, we will sometimes use the convention that $\mathbf{x} = \mathbf{n}a$ and $t = \tau\delta t$, where $\mathbf{n} \in \mathbb{Z}^d$ and $\tau \in \mathbb{Z}$ are the spatial lattice and time coordinates respectively. For simplicity of notation, we will take the spatial lattices to be infinite, but everything extends to finite lattices (with periodic boundary conditions), which is obviously necessary for simulations in practice.

Of course, even though spacetime is now discrete, the field operators at each site still describe continuous degrees of freedom. In practice, for simulations on quantum computers composed of qubits (as opposed to continuous variable modes) the on-site field degrees of freedom themselves would still have to be discretized and truncated as in, e.g., [9]. It seems naively that this would require a huge number of qubits to get an accurate simulation, but in reality truncating the degrees of freedom may not be as costly as we might imagine [38]. Furthermore, an intriguing way to avoid discretizing the field at all is to use continuous variables to store the field modes. This promising idea was explored in [13], which built on a protocol in [40] that allows the implementation of a local cubic gate, an idea that extends to local quartic gates [13]. Nevertheless, how exactly the on-site field operators are discretized will not be our concern here. Instead, we will focus on the dynamics of the field operators with the understanding that a suitable representation of the fields tailored to the architecture of the quantum simulator can be chosen when necessary.

A. Strang-split circuit for scalar field theory

So we want to discretize scalar field theory in terms of a local unitary circuit. There are many possible circuits that have the right continuum limit, but for our first example we choose a circuit coming from Strang splitting (a special case of a Suzuki-Trotter decomposition [41]) the evolution operator of the lattice QFT, $\exp(-iH_{\text{latt}}\delta t)$. The main departure from conventional quantum simulation algorithms for QFT is that we fix the timestep $\delta t = \kappa a$, where κ is a constant. To ensure that the particles arising from solving the free model have real energies (see appendix C), we ought to restrict the values that κ can take. For example, we in one dimensional space, we take $\kappa \lesssim 1/2$. However, to simply maintain the equivalence with the discrete-time path integral formulation of

lattice QFT, $\kappa = 1$ will be sufficient.

The circuit evolving the system over one timestep is

$$U = e^{-iH_X\delta t/2} e^{-iH_P\delta t} e^{-iH_X\delta t/2}, \quad (8)$$

where H_X and H_P were defined in equation (7). Notice that each individual term $e^{-iH_X\delta t/2}$ or $e^{-iH_P\delta t}$ is a product of commuting local unitaries. Thus the unitary applied over each timestep is a finite-depth local unitary circuit.

One advantage of this particular circuit is that we do not need to think of it as approximating the continuous-time lattice Hamiltonian dynamics, but rather as exactly simulating the path integral in the discrete-time Lagrangian formulation of lattice QFT. This follows because it is straightforward to show that

$$\langle \varphi_f | U^\tau | \varphi_i \rangle = \int \mathcal{D}(\varphi) e^{iS(\varphi)}, \quad (9)$$

where $|\varphi_i\rangle$ and $|\varphi_f\rangle$ are initial and final states at time 0 and time τ respectively. The action $S(\varphi)$ is given by

$$S(\varphi) = \sum_{\nu=0}^{\tau-1} \delta t \sum_{\mathbf{n}} a^d \mathcal{L}(\nu, \mathbf{n}), \quad (10)$$

with

$$\mathcal{L}(\nu, \mathbf{n}) = \frac{(\varphi_{\nu+1, \mathbf{n}} - \varphi_{\nu, \mathbf{n}})^2}{2\delta t^2} - \frac{\mathcal{V}(\varphi_{\nu+1, \mathbf{n}}) + \mathcal{V}(\varphi_{\nu, \mathbf{n}})}{2}, \quad (11)$$

with $\mathcal{V}(\varphi_{\nu, \mathbf{n}})$ containing all spatial derivatives, mass term and the interaction, i.e.,

$$\mathcal{V}(\varphi_{\nu, \mathbf{n}}) = \left[\frac{1}{2} (\nabla_a \varphi_{\nu, \mathbf{n}})^2 + \frac{m^2}{2} \varphi_{\nu, \mathbf{n}}^2 + \frac{\lambda}{4!} \varphi_{\nu, \mathbf{n}}^4 \right], \quad (12)$$

where

$$(\nabla_a \varphi_{\nu, \mathbf{n}})^2 = \sum_{\mathbf{e} \in \mathcal{N}} \left(\frac{\varphi_{\nu, \mathbf{n}+\mathbf{e}} - \varphi_{\nu, \mathbf{n}}}{a} \right)^2, \quad (13)$$

where again \mathcal{N} is the set of lattice basis vectors, i.e., $\mathcal{N} = \{(1, 0, \dots, 0), \dots, (0, \dots, 0, 1)\}$. Here $\varphi_{\nu, \mathbf{n}}$ denotes the classical scalar field at time ν at position \mathbf{n} .

The proof of equation (9) is standard, although usually given in the Euclidean formulation with imaginary time (and with periodic boundary conditions in time) [42]. For completeness, we give the full argument in appendix B. From the perspective of lattice QFT, U is the real-time transfer matrix. Note the symmetrized form of the potential \mathcal{V} in the Lagrangian. The interesting point for us is that the real-time transfer matrix is exactly a local quantum circuit.

By choosing a different circuit, e.g., the first-order Trotter decomposition of H_{latt} , given by $U_{\text{Trott}} = e^{-iH_P\delta t} e^{-iH_X\delta t}$, we get a more conventional Lagrangian:

$$\mathcal{L}(\nu, \mathbf{n}) = \frac{(\varphi_{\nu+1, \mathbf{n}} - \varphi_{\nu, \mathbf{n}})^2}{2\delta t^2} - \mathcal{V}(\varphi_{\nu, \mathbf{n}}). \quad (14)$$

However, we would expect that the Strang-split circuit would converge faster to the continuum limit. Another advantage to Strang splitting is that we not only get more accuracy compared to U_{Trott} , but we do it with only one additional layer of unitary gates to implement since

$$U^\tau = e^{-iH_X \delta t/2} (U_{\text{Trott}})^{\tau-1} e^{-iH_P \delta t} e^{-iH_X \delta t/2}, \quad (15)$$

i.e., U_{Trott}^τ consists of 2τ alternating layers like $e^{-iH_P \delta t}$, whereas U^τ consists of $2\tau + 1$.

As we saw above, the advantage of the circuit U is that we get exactly the dynamics described by the discrete-time path integral. In other words, we can simulate discrete-time Lagrangian lattice QFT with zero error, although in practice there will be errors due to imperfect gates. Furthermore, it is straightforward to incorporate improved actions. Note that in current experiments, due to the difficulty in implementing many gates in practice, protocols are limited to the first or second order (Strang-split) Trotter decomposition. In fact, there is sometimes a minimal timestep in experiments [23]. Thus, it makes sense to consider the discrete-time Lagrangian formalism of lattice QFT when simulating QFT on a quantum computer, which, using the circuit here, has the practical benefit of having a timestep with $\delta t = a$.

B. Continuum limit in the free case

In the free case with $\lambda = 0$, it is straightforward to take the continuum limit. Although we already know, via the connection with lattice QFT, that the Strang-split circuit will have the right continuum limit, we can directly verify this in a way that also extends to the alternate circuit we consider in section III D. The circuit evolving the system over one timestep is

$$U_0 = W_X^0 W_P W_X^0, \quad (16)$$

where again each individual W_X^0 or W_P is a product of commuting local unitaries:

$$W_P = \prod_{\mathbf{n} \in \mathbb{Z}^d} \exp\left[\frac{-i\kappa}{2} P_{\mathbf{n}}^2\right]$$

$$W_X^0 = \prod_{\mathbf{n} \in \mathbb{Z}^d} \exp\left[\frac{-i\kappa}{4} \left([2d + \mu^2] X_{\mathbf{n}}^2 - 2 \sum_{\mathbf{e} \in \mathcal{N}} X_{\mathbf{n}+\mathbf{e}} X_{\mathbf{n}}\right)\right]. \quad (17)$$

Let us see how these unitaries act. First, W_P leaves $P_{\mathbf{n}}$ invariant and W_X^0 leaves $X_{\mathbf{n}}$ invariant. So the non trivial effects of the operators are

$$W_X^0 P_{\mathbf{n}} W_X^0 = P_{\mathbf{n}} - \kappa(d + \mu^2/2) X_{\mathbf{n}} + \frac{\kappa}{2} \sum_{\mathbf{e} \in \mathcal{N}} (X_{\mathbf{n}+\mathbf{e}} + X_{\mathbf{n}-\mathbf{e}})$$

$$W_P^\dagger X_{\mathbf{n}} W_P = X_{\mathbf{n}} + \kappa P_{\mathbf{n}}. \quad (18)$$

To take the continuum limit and for solving the circuits, it will be useful to switch to momentum space.

For any operators $A_{\mathbf{n}}$, we define their momentum space representation via

$$A(\mathbf{p}) = a^d \sum_{\mathbf{n} \in \mathbb{Z}^d} e^{-i\mathbf{p} \cdot \mathbf{n} a} A_{\mathbf{n}}, \quad (19)$$

where \mathbf{p} denotes a momentum vector, with components satisfying $p_i \in (-\pi/a, \pi/a]$. Next we need the identity

$$a^d \sum_{\mathbf{n} \in \mathbb{Z}^d} e^{-i\mathbf{p} \cdot \mathbf{n} a} A_{\mathbf{n}+\mathbf{m}} = e^{i\mathbf{p} \cdot \mathbf{m} a} A(\mathbf{p}). \quad (20)$$

Then we get that

$$W_X^{0\dagger} P(\mathbf{p}) W_X^0 = P(\mathbf{p}) + \kappa \left[\sum_{i=1}^d \cos(p_i a) - d - \mu^2/2 \right] X(\mathbf{p})$$

$$W_P^\dagger X(\mathbf{p}) W_P = X(\mathbf{p}) + \kappa P(\mathbf{p}). \quad (21)$$

Using equation (16), we find that the evolution in momentum space is

$$U_0^\dagger X(\mathbf{p}) U_0 = c(\mathbf{p}) X(\mathbf{p}) + \kappa P(\mathbf{p})$$

$$U_0^\dagger P(\mathbf{p}) U_0 = c(\mathbf{p}) P(\mathbf{p}) + \frac{c(\mathbf{p})^2 - 1}{\kappa} X(\mathbf{p}). \quad (22)$$

where we have introduced

$$c(\mathbf{p}) = 1 + \kappa^2 \left[\sum_{i=1}^d \cos(p_i a) - d - \mu^2/2 \right]. \quad (23)$$

It will be helpful to note how $c(\mathbf{p})$ behaves. For small momenta, with each $p_i \ll 1/a$, we can Taylor expand to see that $c(\mathbf{p}) = 1 - (\mathbf{p}^2 + m^2) \delta t^2/2 + O(a^4)$.

In terms of the field operators, for small momentum, we see that

$$U_0^\dagger \phi(\mathbf{p}) U_0 = \phi(\mathbf{p}) + \pi(\mathbf{p}) \delta t + O(a^2)$$

$$U_0^\dagger \pi(\mathbf{p}) U_0 = \pi(\mathbf{p}) - \delta t (\mathbf{p}^2 + m^2) \phi(\mathbf{p}) + O(a^2). \quad (24)$$

This allows us to find time derivatives in the continuum limit. In the Heisenberg picture we have, e.g., $\phi(t + \delta t, \mathbf{p}) = U_0^\dagger \phi(t, \mathbf{p}) U_0$. Then we can find the time derivative of the field as the lattice spacing $a \propto \delta t$ goes to zero:

$$\partial_t \phi(t, \mathbf{p}) = \lim_{a \rightarrow 0} \frac{U_0^\dagger \phi(t, \mathbf{p}) U_0 - \phi(t, \mathbf{p})}{\delta t}. \quad (25)$$

This gives us back exactly the equations of motion for the Klein-Gordon field in momentum space:

$$\partial_t \phi(t, \mathbf{p}) = \pi(t, \mathbf{p})$$

$$\partial_t \pi(t, \mathbf{p}) = -(\mathbf{p}^2 + m^2) \phi(t, \mathbf{p}). \quad (26)$$

So we see that for low momenta, or equivalently physics on length scales that are large compared to the lattice spacing, we have the usual scalar field dynamics.

C. Solution of the free circuits

We can solve the free circuit U_0 , with the full details being given in appendix C. Actually, for the Strang-split circuit, the solution is known from lattice QFT in the Wick-rotated imaginary time setting. Nevertheless, with a little modification, the method also applies to the new circuit we will consider in section III D. The solution entails finding creation and annihilation operators, satisfying

$$[b_{\mathbf{p}}, b_{\mathbf{q}}^\dagger] = (2\pi)^d \delta^{(d)}(\mathbf{p} - \mathbf{q}). \quad (27)$$

These also satisfy

$$U_0^\dagger b_{\mathbf{p}} U_0 = e^{-i\theta(\mathbf{p})\delta t} b_{\mathbf{p}}. \quad (28)$$

Here $\theta(\mathbf{p})$ plays the role of the energy of a particle and is defined by

$$e^{-i\theta(\mathbf{p})\delta t} = c(\mathbf{p}) - i\sqrt{1 - c(\mathbf{p})^2}, \quad (29)$$

where $c(\mathbf{p})$ was introduced in equation (23). The function $\theta(\mathbf{p})$ is positive and is gapped above zero. Furthermore,

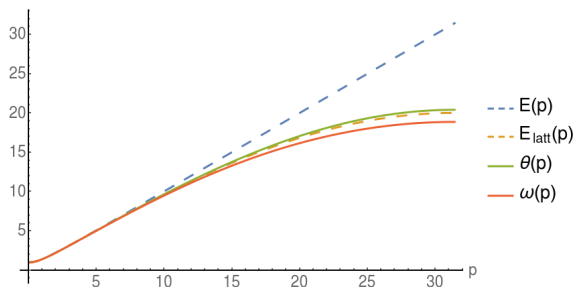


FIG. 1: Comparison of different energy functions in $d = 1$. $E(p) = \sqrt{p^2 + m^2}$ is the usual continuum energy dispersion relation, whereas $E_{\text{latt}}(p) = \sqrt{m^2 + 4 \sin^2[pa/2]/a^2}$ is the dispersion relation for the lattice Hamiltonian with $\lambda = 0$ from section II. In contrast, in discrete time there are two functions that play the role of energy: $\theta(p)$ appears in the phase picked up by annihilation operators, whereas $\omega(p)$ appears in the denominator in equal-time correlation functions. In continuum and Hamiltonian lattice QFT, both roles are played by $E(p)$ and $E_{\text{latt}}(p)$ respectively. Here we plot all of these functions with the lattice spacing taken to be 0.1 and $m = 1$. The plot is over half the momentum range $[0, \pi/a]$ since it is symmetric. Note that we have chosen $\kappa = 1/3$, i.e., $\delta t = a/3$ for our circuit. The figure shows that $\omega(p)$ is a slightly worse approximation to $E(p)$ than $E_{\text{latt}}(p)$, whereas $\theta(p)$ is a slightly better approximation.

we choose κ such that $\theta(\mathbf{p})$ is bounded above by $\pi/(2\delta t)$, which requires that

$$\kappa^2 < \frac{2}{4d + \mu^2}. \quad (30)$$

Note that slightly bigger values for κ are possible, as discussed in appendix C, in which case the constraint is

that we want the energies $\theta(\mathbf{p})$ to be real. Also, as we would hope, for small a , we have

$$e^{-i\theta(\mathbf{p})\delta t} = 1 - iE(\mathbf{p})\delta t + \mathcal{O}(\delta t^2), \quad (31)$$

where $E(\mathbf{p}) = \sqrt{\mathbf{p}^2 + m^2}$. We see in appendix C that we can write our field operators in the Heisenberg picture as

$$\begin{aligned} \phi(x) &= \int \frac{d^d p}{(2\pi)^d} \frac{1}{\sqrt{2\omega(\mathbf{p})}} (e^{-ip_s \cdot x} b_{\mathbf{p}} + e^{ip_s \cdot x} b_{\mathbf{p}}^\dagger) \\ \pi(x) &= -i \int \frac{d^d p}{(2\pi)^d} \sqrt{\frac{\omega(\mathbf{p})}{2}} (e^{-ip_s \cdot x} b_{\mathbf{p}} - e^{ip_s \cdot x} b_{\mathbf{p}}^\dagger), \end{aligned} \quad (32)$$

where we are using the notation $x^\mu = (t, \mathbf{x}) = (\tau\delta t, \mathbf{n}a)$ and $p_s^\mu = (\theta(\mathbf{p}), \mathbf{p})$, with $p_s \cdot x = \theta(\mathbf{p})t - \mathbf{p} \cdot \mathbf{x}$. We also have

$$\omega(\mathbf{p}) = \frac{\sin[\theta(\mathbf{p})\delta t]}{\delta t}. \quad (33)$$

The free circuit vacuum is given by $|0\rangle$, the state annihilated by all $b_{\mathbf{p}}$. Furthermore, vacuum correlations are described by the equal-time propagator:

$$\langle 0 | \phi(x) \phi(y) | 0 \rangle = \int \frac{d^d p}{(2\pi)^d} \frac{e^{i\mathbf{p} \cdot (\mathbf{x} - \mathbf{y})}}{2\omega(\mathbf{p})}, \quad (34)$$

where $x^0 = y^0$. As $\omega(\mathbf{p}) \rightarrow E(\mathbf{p})$ for small $\mathbf{p}a$, the circuit equal-time propagator reproduces the continuum version for small momenta. This means that the circuit vacuum approximates the continuum vacuum well at length scales that are large compared to a .

In Hamiltonian lattice QFT or continuum QFT, the energy that appears in the exponents in the field operators and in the factor after the integral in the field operator are the same. In contrast, here (and in the discrete-time Lagrangian formalism of lattice QFT [42]) we have the discrete energy $\theta(\mathbf{p})$ in the exponent and a different factor $\omega(\mathbf{p}) = \sin[\theta(\mathbf{p})\delta t]/\delta t$ in the denominator in the integral. Nevertheless, for small lattice momenta, both coincide, and the expressions look like the familiar continuum field operators. These two functions, $\theta(\mathbf{p})$ and $\omega(\mathbf{p})$, are plotted in figure 1.

We can also find the discrete spacetime Feynman propagator:

$$D_F(x - y) = \langle 0 | \mathcal{T}[\phi(x)\phi(y)] | 0 \rangle \quad (35)$$

where \mathcal{T} is the time-ordering operator. We show in appendix D that the Feynman propagator can be written as

$$D_F(x - y) = \frac{\delta t^2}{2} \int \frac{d^D p}{(2\pi)^D} \frac{ie^{-ip \cdot (x - y)}}{\cos[\theta_\varepsilon(\mathbf{p})\delta t] - \cos[p_0\delta t]}, \quad (36)$$

where $D = d + 1$ and we have $\theta_\varepsilon(\mathbf{p}) = \theta(\mathbf{p}) - i\varepsilon$. One should take the limit of $\varepsilon \rightarrow 0$ in calculations. Note that from here on, unless otherwise specified, momentum integrals range over $(-\pi/\delta t, \pi/\delta t) \times (-\pi/a, \pi/a)^d$, where

the first factor corresponds to the p_0 integral. In fact, we can also choose our $i\varepsilon$ prescription slightly differently to get

$$D_F(x-y) = \frac{\delta t^2}{2} \int \frac{d^D p}{(2\pi)^D} \frac{i e^{-ip \cdot (x-y)}}{\cos[\theta(\mathbf{p})\delta t] - \cos[p_0\delta t] + i\varepsilon}. \quad (37)$$

In the limit as $a \rightarrow 0$, we recover the usual Feynman propagator. The momentum-space propagator is

$$D_F(p) = \frac{\delta t^2}{2} \frac{i}{\cos[\theta(\mathbf{p})\delta t] - \cos[p_0\delta t] + i\varepsilon}. \quad (38)$$

Everything in this section applies to the new circuit we will consider in the following section: only the form of $\theta(\mathbf{p})$ will be different, and we also take $\delta t = a$.

D. Shift circuit for scalar field theory

Here we give a second circuit for scalar field theory. For want of a better name, we will call this the shift circuit. The motivation for the circuit we will choose is that, with $m = 0$ in $d = 1$, it is a natural discretization of the dynamics of the continuum field. To see how this works, let us make a brief digression to continuous spacetime. Then we introduce left and right-moving fields, given by

$$\begin{aligned} \pi_L(\mathbf{x}) &= \frac{1}{2} (\pi(\mathbf{x}) + \partial_{\mathbf{x}}\phi(\mathbf{x})) \\ \pi_R(\mathbf{y}) &= \frac{1}{2} (\pi(\mathbf{x}) - \partial_{\mathbf{x}}\phi(\mathbf{x})), \end{aligned} \quad (39)$$

where \mathbf{x} is just a one-dimensional vector since $d = 1$. The dynamics in the Heisenberg picture for the free field is simply

$$\begin{aligned} \pi_L(t, \mathbf{x}) &= \pi_L(0, \mathbf{x} + t) \\ \pi_R(t, \mathbf{x}) &= \pi_R(0, \mathbf{x} - t). \end{aligned} \quad (40)$$

In other words, as the name suggests left-moving fields move left and right-moving fields move right.

Returning to discrete spacetime, the quantum circuit we introduce below is a simple discretization of this when restricted to $d = 1$ and $m = 0$ with $\lambda = 0$. The evolution operator in general takes the form

$$U = W_X W_P W_X, \quad (41)$$

but with a new choice of W_X and W_P , given by

$$\begin{aligned} W_X &= \prod_{\mathbf{n} \in \mathbb{Z}^d} \exp \left[\frac{iM}{2^D} \sum_{\mathbf{e} \in N} X_{\mathbf{n}} X_{\mathbf{n}+\mathbf{e}} + \frac{\Lambda}{4!} X_{\mathbf{n}}^4 \right] \\ W_P &= \prod_{\mathbf{n} \in \mathbb{Z}^d} \exp \left[\frac{i\pi}{4} (X_{\mathbf{n}}^2 + P_{\mathbf{n}}^2) \right]. \end{aligned} \quad (42)$$

Here $M = 1 - m^2 a^2 / 2$, where m is the mass, and N is the set of lattice vectors \mathbf{e} with components $e_i = \pm 1$. In

this case, we have $\delta t = a$. In the absence of interactions, i.e., with $\Lambda = 0$, we denote the evolution operator by U_0 .

In $d = 1$, we can define lattice left-moving and right-moving fields $\pi_{L,n}$ and $\pi_{R,n}$ by

$$\begin{aligned} \pi_{L,n} &= \frac{1}{2} \left(\pi_n + \frac{\phi_{n+1} - \phi_{n-1}}{2a} \right) \\ \pi_{R,n} &= \frac{1}{2} \left(\pi_n - \frac{\phi_{n+1} - \phi_{n-1}}{2a} \right), \end{aligned} \quad (43)$$

which obey the commutation relations

$$\begin{aligned} [\pi_{L,m}, \pi_{R,n}] &= 0 \\ [\pi_{L,m}, \pi_{L,n}] &= -\frac{i}{4a^2} (\delta_{m,n+1} - \delta_{m,n-1}) \\ [\pi_{R,m}, \pi_{R,n}] &= \frac{i}{4a^2} (\delta_{m,n+1} - \delta_{m,n-1}). \end{aligned} \quad (44)$$

The operators $\pi_{L,n}$ and $\pi_{R,n}$ tend in the continuum limit to the continuum right and left-movers $\pi_R(\mathbf{x})$ and $\pi_L(\mathbf{x})$ with the correct commutation relations. Furthermore, with $m = 0$ the unitary U_0 shifts $\pi_{L,n}$ left and $\pi_{R,n}$ right over each timestep, i.e.,

$$\begin{aligned} U_0^\dagger \pi_{L,m} U_0 &= \pi_{L,m+1} \\ U_0^\dagger \pi_{R,m} U_0 &= \pi_{R,m-1}, \end{aligned} \quad (45)$$

which is a simple discretization of equation (40).

More generally, for arbitrary spatial dimension and non-zero mass, in momentum space the quantum-circuit dynamics is again given by

$$\begin{aligned} U_0^\dagger \phi(\mathbf{p}) U_0 &= c(\mathbf{p}) \phi(\mathbf{p}) + a\pi(\mathbf{p}) \\ U_0^\dagger \pi(\mathbf{p}) U_0 &= c(\mathbf{p}) \pi(\mathbf{p}) - \frac{c(\mathbf{p})^2 - 1}{a} \phi(\mathbf{p}), \end{aligned} \quad (46)$$

but now we have

$$c(\mathbf{p}) = M \prod_{i=1}^d \cos(p_i a). \quad (47)$$

Both energy functions $\theta(\mathbf{p})$ and $\omega(\mathbf{p})$ can be found as described in section III C. Furthermore, the field operators and the propagator have the same form as those in equations (32) and (37) only with a different $\theta(\mathbf{p})$ function.

However, there is a slight problem with this model. Recall that the equal-time propagator is

$$\langle 0 | \phi(x) \phi(y) | 0 \rangle = \int \frac{d\mathbf{p}}{2\pi} \frac{e^{i\mathbf{p} \cdot (\mathbf{x}-\mathbf{y})}}{2\omega(\mathbf{p})}, \quad (48)$$

where $x^0 = y^0$. Note that $\omega(\mathbf{p}) = \sin[\theta(\mathbf{p})a]/a$ has small values, not only for $|\mathbf{p}a| \ll 1$, but also for high momenta $|\mathbf{p}a| \sim \pi$, which is analogous to fermion doubling: the high-momentum particles contribute as if there is a second type of particle present. Figure 2 shows a plot of $\omega(\mathbf{p})$ and $\theta(\mathbf{p})$ for this model in $d = 1$, compared to

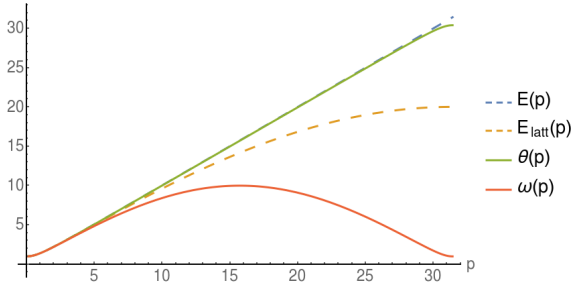


FIG. 2: Comparison of energies of the Shift circuit in $d = 1$. $E(p) = \sqrt{p^2 + m^2}$ is the continuum dispersion relation, and $E_{\text{latt}}(p) = \sqrt{m^2 + 4 \sin^2[pa/2]/a^2}$ is the dispersion relation for the lattice Hamiltonian with $\lambda = 0$ from section II. Again, for the Shift circuit, there are two functions that play the role of energy, $\theta(p)$ appears in the phase picked up by annihilation operators, and $\omega(p)$ appears in equal-time correlation functions. These are plotted with lattice spacing taken to be 0.1 and $m = 1$. The plot is over half the momentum range $[0, \pi/a]$ since it is symmetric. For this model $\delta t = a$. In this case, $\omega(p)$ is a poor approximation to $E(p)$ for large p , but, on the other hand, $\theta(p)$ is staggeringly close to $E(p)$.

the continuum energy $E(\mathbf{p})$. Interestingly, $\theta(\mathbf{p})$ is an extremely good approximation to $E(\mathbf{p})$, whereas $\omega(\mathbf{p})$ becomes a poor approximation for large p . To mitigate this problem, we will modify the interaction from the point interaction $\phi_{\mathbf{n}}^4$ to something averaged over a few sites thus averaging out high momentum contributions to scattering amplitudes. We look at this problem and its solution in more detail in section IV B. Another option would be to modify the free circuit along the lines of Wilson's solution to the fermion doubling problem, i.e., by introducing an artificial mass term that only affects high momentum particles.

IV. INTERACTING FIELDS

In cases where we do not have a simple correspondence with Lagrangian lattice QFT, it is still possible to include interactions and even do perturbation theory. In particular, this applies to the Shift circuit of section III D. Even in the case of the Strang-split circuit of section III A, the discrete-time formalism below can be applied to derive the Feynman rules. The ideas here may also have other uses in quantum circuit simulations of other field theories when there is no connection to a path integral or to quantum cellular automata more generally.

To include interactions in our model, we can add further unitaries to the free dynamics:

$$U = U_{\text{int}}^{1/2} U_0 U_{\text{int}}^{1/2} \quad (49)$$

where U_0 is the unitary evolution operator for the free theory, and $U_{\text{int}} = e^{-iV}$ is the interaction unitary, where V is essentially the analogue of the interaction term in a Hamiltonian. Note that in the cases we have considered,

the unitary is already in this form since we can factor out $U_{\text{int}}^{1/2} = e^{-iV/2}$ with

$$V = a^d \delta t \frac{\lambda}{4!} \sum_{\mathbf{n} \in \mathbb{Z}^d} \phi_{\mathbf{n}}^4. \quad (50)$$

This follows because, in both cases, i.e., equations (8) and (42), all terms in W_X commute, so $W_X = W_X^0 e^{-iV/2}$.

At this point, it is useful to introduce the interaction picture, where in a rough sense operators evolve via the free dynamics and states evolve via the rest. More precisely, for operators in the interaction picture, we have

$$A_I(\tau) = U_0^{\dagger \tau} A_S U_0^\tau, \quad (51)$$

where $\tau \in \mathbb{Z}$ and A_S denotes an operator in the Schrödinger picture. To find the evolution operator for states, we note that physical quantities cannot depend on which picture we use, so we require that

$$\langle \psi_f | U^{\dagger \tau} A_S U^\tau | \psi_i \rangle = \langle \psi_f | [U^{\dagger \tau} U_0^\tau] A_I(\tau) [U_0^{\dagger \tau} U^\tau] | \psi_i \rangle, \quad (52)$$

where both $|\psi_i\rangle$ and $|\psi_f\rangle$ are states in the Schrödinger picture. Thus, the evolution operator for states in the interaction picture from time 0 to time τ is

$$\begin{aligned} U_I(\tau, 0) &= U_0^{\dagger \tau} U^\tau \\ &= U_0^{\dagger \tau} (U_{\text{int}}^{1/2} U_0 U_{\text{int}}^{1/2})^\tau \\ &= U_0^{\dagger \tau} U_{\text{int}}^{1/2} U_0 U_{\text{int}}^{1/2} (U_{\text{int}}^{1/2} U_0 U_{\text{int}}^{1/2})^{\tau-1} \\ &= U_{\text{int},I}^{1/2}(\tau) U_{\text{int},I}^{1/2}(\tau-1) U_0^{\dagger \tau-1} (U_{\text{int}}^{1/2} U_0 U_{\text{int}}^{1/2})^{\tau-1} \\ &= U_{\text{int},I}^{1/2}(\tau) U_{\text{int},I}(\tau-1) \dots U_{\text{int},I}(1) U_{\text{int},I}^{1/2}(0), \end{aligned} \quad (53)$$

where $U_{\text{int},I}(\tau)$ is the operator U_{int} in the interaction picture, i.e.,

$$U_{\text{int},I}(\tau) = U_0^{\dagger \tau} U_{\text{int}} U_0^\tau = e^{-iV_I(\tau)}. \quad (54)$$

The interaction picture evolution operator for states from time τ_1 to time τ_2 can then be written as

$$U_I(\tau_2, \tau_1) = \mathcal{T} \left[\exp \left(-i \left[\frac{1}{2} V_I(\tau_2) + \sum_{\nu=\tau_1-1}^{\tau_2-1} V_I(\nu) + \frac{1}{2} V_I(\tau_1) \right] \right) \right]. \quad (55)$$

This looks the same as the continuum expression, except that instead of an integral over time, we have a sum over discrete times and we have the slightly different boundary conditions at times τ_1 and τ_2 . Since we will take the limit as these go to infinity, this is unimportant.

Note that this is completely general, so we could of course consider different interaction terms like $\phi_{\mathbf{n}}^3$. And the idea applies to other analogous discretizations of QFT

where there is some U_0 that we can solve and some non-trivial U_{int} . Also, note that the alternate prescription for adding interactions analogous to the first-order Trotter decomposition $U = U_0 U_{\text{int}}$ (or $U = U_{\text{int}} U_0$) works in a similar way, but we get the interaction-picture evolution operator

$$U_I(\tau_2, \tau_1) = \mathcal{T} \left[\exp \left(-i \sum_{\nu=\tau_1}^{\tau_2-1} V_I(\nu) \right) \right]. \quad (56)$$

Because Strang splitting is typically more accurate than the first-order Trotter decomposition, one would expect that the symmetric way of including the interaction would be more accurate in practice. Whichever we choose, the Feynman rules of the next section are the same. It may be possible to extend these formulas to higher order Suzuki-Trotter decompositions in a similar way, though the expressions would be more complex.

A. Feynman rules

In this section, we will give the Feynman rules for our circuits. The ideas have the potential to apply to alternative quantum circuits discretizing QFTs that have no obvious connection to Lagrangians or even Hamiltonians. Getting Feynman rules giving correct descriptions of physical processes from a proposed circuit would then serve as a guide as to whether the proposed circuits are useful discretizations for quantum simulations of a QFT.

The arguments we use to get the Feynman rules are given in appendix E and are almost identical to those in continuum QFT (via canonical quantization), which can be found in, e.g., [43, 44]. We will not give a rigorous derivation along the lines of an LSZ reduction formula or, e.g., a discrete-time version of the Gell-Mann and Low theorem [45]. Instead, we will start with intuitive notions of asymptotically free states that scatter. With that in mind, we define the scattering matrix to be

$$S = \lim_{\tau \rightarrow \infty} U_I(\tau, -\tau), \quad (57)$$

which is analogous to the continuum expression. The goal is then to approximate scattering amplitudes of the form

$$\langle f | S | i \rangle, \quad (58)$$

where $|i\rangle$ and $|f\rangle$ are initial and final states, e.g., for two incoming particles, we would ideally have

$$|i\rangle = \sqrt{2\omega(\mathbf{p})} \sqrt{2\omega(\mathbf{q})} b_{\mathbf{p}}^\dagger b_{\mathbf{q}}^\dagger |0\rangle. \quad (59)$$

Here are the rules for calculating $\langle f | S | i \rangle$. A sketch of their derivation is given in appendix E.

1. Draw all possible amputated and connected diagrams with the right number of incoming and outgoing legs.

2. Assign a directed momentum to each line, with energy and momentum conservation at each vertex.
3. Each internal line picks up a momentum-space propagator $D_F(p)$.
4. Each vertex gets a factor of $-i\lambda$.
5. Integrate over all undetermined momenta via

$$\int \frac{d^D p}{(2\pi)^D}.$$

6. Divide by the symmetry factor of each diagram.

Note that the symmetry factor is the same as that arising in conventional perturbation theory in QFT for ϕ^4 theory with the conventional $\lambda/4!$ factor. The only differences are that the propagator $D_F(p)$ has a different form compared to the continuum, and energy-momentum integrals are over $(-\pi/\delta t, \pi/\delta t) \times (-\pi/a, \pi/a)^d$. These modifications are not dissimilar to those for the Feynman rules in lattice QFT [4]. Indeed, for the Strang-split circuit, these are exactly the same as in discrete-time Lagrangian lattice QFT. For the Shift circuit, which has no obvious lattice QFT analogue, we have a new propagator.

B. One loop correction to mass

For the Strang-split circuit, we know that we have a good regulator, but it is not completely clear that this is true for the Shift circuit. So, for the case of the Shift circuit, let us put the Feynman rules to work to calculate the first order correction to the mass of a particle in $D = 1 + 1$. This corresponds to the diagram in figure 3. (Actually, this is not an amputated diagram. In fact, it is

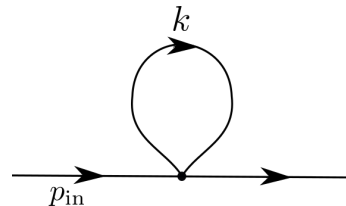


FIG. 3: One-loop correction to the propagator in the presence of interactions.

necessary to compute this diagram when calculating how the propagator is modified in the presence of interactions in order to apply the LSZ formula.)

Via the Feynman rules, we get

$$\begin{aligned} \Pi_{\text{Shift}}(p_{\text{in}}^2) &= -i\lambda \frac{1}{2} \int \frac{d^2 k}{(2\pi)^2} \frac{\delta t^2}{2} \frac{i}{\cos[\theta_\varepsilon(k_1)\delta t] - \cos[k_0\delta t]} \\ &= \frac{\lambda}{2} \int \frac{dk_1}{2\pi} \frac{\delta t}{2} \frac{1}{\sin[\theta(k_1)\delta t]} \\ &= \frac{\lambda}{4} \int \frac{dk_1}{2\pi} \frac{\delta t}{\sqrt{1 - c(k_1)^2}}, \end{aligned} \quad (60)$$

where the factor of $1/2$ in the first line comes from the symmetry factor of the diagram, and we got the third line by using the definition of $e^{-i\theta(k_1)\delta t}$ in equation (29). We show in appendix F that

$$\Pi_{\text{Shift}}(p_{\text{in}}^2) = \frac{\lambda}{2\pi} \ln\left(\frac{1}{ma}\right) + \text{finite}. \quad (61)$$

This is actually too big by a factor of two compared to other regulators, e.g., continuum QFT $\Pi_{\text{cont}}(p_{\text{in}}^2)$ with a momentum cutoff Λ or the Strang-split circuit $\Pi_{\text{Strang}}(p_{\text{in}}^2)$. These give

$$\begin{aligned} \Pi_{\text{cont}}(p_{\text{in}}^2) &= \frac{\lambda}{4\pi} \ln\left(\frac{\Lambda}{m}\right) + \text{finite} \\ \Pi_{\text{Strang}}(p_{\text{in}}^2) &= \frac{\lambda}{4\pi} \ln\left(\frac{\Delta}{ma}\right) + \text{finite}, \end{aligned} \quad (62)$$

where $\Delta \ll 1$ is a constant. These are also calculated in appendix F. The problem is that the Shift circuit has those high momentum modes with small values of $\omega(p) = \sin[\theta(p)a]/a$. These contribute to the Feynman diagram calculations as if there is a second type of particle present. To get around this, we can consider the modified interaction term

$$V = a^D \frac{\lambda}{4!} \sum_{\mathbf{n} \in \mathbb{Z}^d} \left(\sum_{\mathbf{e} \in \mathcal{K}} w(\mathbf{e}) \phi_{\mathbf{n}+\mathbf{e}} \right)^4, \quad (63)$$

where \mathcal{K} is the set of all vectors with components in $\{-1, 0, 1\}$ and $w(\mathbf{e}) = v(e_1) \times \dots \times v(e_d)$ with $v(-1) = v(1) = 1/4$ and $v(0) = 1/2$. This choice modifies the Feynman rules slightly, so that the vertex factor depends on the momentum flowing in or out, but, as shown in appendix F, we then get the new value for the diagram

$$\Pi_{\text{Shift}}(p_{\text{in}}^2) = \frac{\lambda}{4\pi} \ln\left(\frac{1}{ma}\right) + \text{finite} \quad (64)$$

as long as $p_{\text{in}} \ll 1/a$. This is the desired result for the diagram with the same divergence as for other regulators in equation (62).

Of course, to actually do a perturbative calculation in ϕ^4 theory, there are much more convenient regulators than the Shift circuit we have introduced, such as dimensional regularization. The point is that this circuit, as well as the Strang-split circuit, captures the right physics, despite choosing $\delta t \propto a$. Nevertheless, in principle even for the Shift circuit one could also perform perturbative renormalization, which is a crucial part of understanding the continuum limit in the presence of weak interactions.

V. LOCAL CIRCUIT FOR NON-ABELIAN GAUGE THEORY

Based on the correspondence between the local circuit of section III A and the discrete-time path integral expression for amplitudes in ϕ^4 theory, it makes sense to

ask whether other path integral amplitudes have exact decompositions in terms of local circuits. One case where this is possible is for pure non-abelian gauge theory on the lattice, which, despite the absence of matter, is an interacting theory. The basic idea we will use here is simple: the path integral can of course be written in terms of a real-time transfer matrix. The interesting point is that the transfer matrix is actually a finite-depth local quantum circuit. We can think of this as a quantum cellular automaton describing pure gauge theory.

Here we will not focus on the details of what scheme is used to discretize the on-site field operators themselves in order to represent them in terms of qubits, but we will return to this question at the end. It may also make sense to represent the fields on a continuous-variable system for simulation via photonic circuits.

Again we have a discrete spatial lattice, but now we have Hilbert spaces associated to links between lattice sites. Recall that we may denote lattice sites by \mathbf{x} with components in $a\mathbb{Z}$, and let \mathbf{e} denote lattice basis vectors, so $\mathbf{e} \in \{(a, 0, \dots, 0), \dots, (0, \dots, 0, a)\}$. The Hilbert space for the link $(\mathbf{x}, \mathbf{x} + \mathbf{e})$ is spanned by the basis $|U_{\mathbf{x},\mathbf{e}}\rangle$, where $U_{\mathbf{x},\mathbf{e}}$ denotes an element of the defining representation of the gauge group \mathcal{G} , which we assume is either $U(1)$ or $SU(n)$. (Non-compact groups like \mathbb{R} can also be considered.) In other words, $U_{\mathbf{x},\mathbf{e}}$ corresponds to a matrix of real numbers $U_{\mathbf{x},\mathbf{e}}^{ab}$, where a and b are the matrix indices corresponding to the indices of the group representation, e.g., for $SU(n)$, these run from 1 to n , whereas for $U(1)$ there is only a single element. These basis states satisfy

$$\begin{aligned} \langle V_{\mathbf{x},\mathbf{e}} | U_{\mathbf{x},\mathbf{e}} \rangle &= \delta(V_{\mathbf{x},\mathbf{e}}, U_{\mathbf{x},\mathbf{e}}) \\ \int dU_{\mathbf{x},\mathbf{e}} |U_{\mathbf{x},\mathbf{e}}\rangle \langle U_{\mathbf{x},\mathbf{e}}| &= \mathbb{1}, \end{aligned} \quad (65)$$

where $dU_{\mathbf{x},\mathbf{e}}$ denotes the normalized Haar measure over the group and $\int dU \delta(U, V) = 1$. We also associate operators $\hat{U}_{\mathbf{x},\mathbf{e}}^{ab}$ to each link (in this section it is convenient to write hats over operators) with

$$\hat{U}_{\mathbf{x},\mathbf{e}}^{ab} |U_{\mathbf{x},\mathbf{e}}\rangle = U_{\mathbf{x},\mathbf{e}}^{ab} |U_{\mathbf{x},\mathbf{e}}\rangle. \quad (66)$$

One important observable is given by the trace of spatial plaquette operators on the lattice. These are defined by

$$\text{tr}[\hat{U}_{\mathbf{p}_s}] = \hat{U}_{\mathbf{x},\mathbf{e}}^{ab} \hat{U}_{\mathbf{x}+\mathbf{e},\mathbf{f}}^{bc} \hat{U}_{\mathbf{x}+\mathbf{f},\mathbf{e}}^{cd} \hat{U}_{\mathbf{x},\mathbf{f}}^{\dagger da}, \quad (67)$$

where the repeated matrix indices are summed, and $\mathbf{p}_s = (\mathbf{x}, \mathbf{x} + \mathbf{e}, \mathbf{x} + \mathbf{e} + \mathbf{f}, \mathbf{x} + \mathbf{f})$ is shorthand for a spatial plaquette. Finally, we may define left shift operators that act on link states via

$$\hat{L}_{\mathbf{x},\mathbf{e}}(V) |U_{\mathbf{x},\mathbf{e}}\rangle = |V^\dagger U_{\mathbf{x},\mathbf{e}}\rangle. \quad (68)$$

Right shift operators can be defined analogously.

Finally, we require that physical states all satisfy Gauss' law. This is equivalent to the statement that they are invariant under spatial gauge transformations:

$$U_{\mathbf{x},\mathbf{e}} \rightarrow \Omega_{\mathbf{x}} U_{\mathbf{x},\mathbf{e}} \Omega_{\mathbf{x}+\mathbf{e}}^\dagger = U_{\mathbf{x},\mathbf{e}}^\Omega, \quad (69)$$

where $\Omega_{\mathbf{x}}$ are all elements of the gauge group. We can define a unitary operator that implements such a gauge transformation on states to be

$$D(\Omega)|U\rangle = |U^\Omega\rangle. \quad (70)$$

Then Gauss' law is just the statement that $D(\Omega)|U\rangle = |U\rangle$ for any Ω .

This all allows us to introduce the real-time (hence unitary) transfer operator \hat{T} , given by

$$\hat{T} = \hat{W}_{\text{el}}\hat{W}_{\text{mag}}, \quad (71)$$

where

$$\begin{aligned} \hat{W}_{\text{mag}} &= \exp\left(-i\frac{2\kappa}{g^2}\sum_{\mathbf{p}_s}\text{Re}\left(\text{tr}[\hat{U}_{\mathbf{p}_s}]\right)\right) \\ \hat{W}_{\text{el}} &= \prod_{\mathbf{x},\mathbf{e}}\int dV_{\mathbf{x},\mathbf{e}}\exp\left(-i\frac{2}{\kappa g^2}\text{Re}\left(\text{tr}[V_{\mathbf{x},\mathbf{e}}]\right)\right)\hat{L}_{\mathbf{x},\mathbf{e}}(V_{\mathbf{x},\mathbf{e}}), \end{aligned} \quad (72)$$

where g is the gauge coupling constant, and $\text{Re}(\text{tr}[A]) = (\text{tr}[A] + \text{tr}[A^\dagger])/2$. Note that the product over plaquettes counts each plaquette only once. The crucial point here is that the terms in the exponents in the definition of W_{mag} all commute since plaquette operators $\hat{U}_{\mathbf{p}_s}$ all commute with each other. As a result, both W_{mag} and W_{el} are finite-depth local quantum unitaries. The depth of W_{el} is one since each unitary acts on a different link, whereas the depth of W_{mag} depends on the lattice dimension because plaquette operators may overlap on links. For example, in $d = 2$ the smallest possible depth is two: the unitaries on plaquettes can be applied in a chess-board pattern. More generally, a circuit depth of $d!$ is sufficient by applying the $d = 2$ protocol for each pair of directions.

The reason for this form of evolution operator in equation (71) is that it is equivalent to a discrete-time path integral with the Wilson action. In other words, given initial and final gauge field configurations obeying Gauss' law, $|U_i\rangle$ and $|U_f\rangle$, it then follows that

$$\langle U_f|\hat{T}^\tau|U_i\rangle = \int \mathcal{D}(U)e^{iS(U)}, \quad (73)$$

where the action $S(U)$ when $\delta t = a$ is given by

$$S(U) = \frac{2}{g^2}\sum_p\text{Re}\left(\text{tr}[U_p]\right), \quad (74)$$

where we have

$$\text{tr}[U_p] = U_{x,e}^{ab}U_{x+e,f}^{bc}U_{x+f,e}^{*cd}U_{x,f}^{*da}, \quad (75)$$

where $p = (x, x + e, x + e + f, x + f)$ is a spacetime plaquette, with x representing a spacetime coordinate and e and f are spacetime lattice basis vectors. The range of the sum is over all spacetime plaquettes on $\{0, \dots, \tau\} \times \mathbb{Z}^d$

except spatial plaquettes at time τ . Finally, the measure is given by

$$\mathcal{D}(U) = \prod_{x,e} dU_{x,e}. \quad (76)$$

The equivalence, i.e., equation (73), is shown in appendix G.

As written here, the unitaries W_{mag} and W_{el} , although local finite-depth circuits, are still opaque. In practice, to simulate this quantum field theory, we would need to represent the link Hilbert spaces and operators on either qubits or continuous variable systems. Once a suitable encoding is chosen, it then makes sense to work to parameterize each unitary in a more convenient manner. One possibility is to use the group theoretic methods from [8] to truncate the link Hilbert spaces in order to represent them on qubits. There are several different but equivalent ways to write W_{el} that may be useful depending on the particular encoding [42].

VI. CONCLUSION AND OUTLOOK

The main take-home message here is that a timestep of $\delta t \sim a$ will be sufficient for quantum simulations of QFT in practice. This is important because there are sometimes lower bounds on the length of time a gate can be applied [23]. Also, in contrast to the the conventional approach in quantum simulation of QFT, namely focusing on the continuous-time Hamiltonian version of lattice QFT, this shows that it is sometimes more natural to use the discrete-time Lagrangian formulation. Furthermore, a priori there is no reason why the continuous-time Hamiltonian formulation of lattice QFT is physically more fundamental than the discrete-time Lagrangian formulation, which puts time and space on a more even footing akin to special relativity.

The connection between path integrals in Euclidean Lagrangian lattice QFT and the imaginary-time transfer matrix is of course well known. The really interesting and useful point for us was that for scalar fields and for non-abelian gauge fields the real-time transfer matrix, and hence the real-time path integral, are exactly equal to finite-depth local quantum circuits with no approximation error. At the moment, however, it seems that a similar trick does not work as nicely for fermions because the transfer matrix does not factor into a finite-depth local circuit for, say, Wilson fermions. So the next question that we hope to address in future work is how best to extend these ideas to, e.g., quantum electrodynamics.

In our setting, it is also straightforward to simulate systems with improved actions, which have been heavily studied in lattice QFT. This prompts a related question: is it possible to see further improvement in simulations by going beyond conventional circuits and instead trying circuits with no obvious connection to lattice QFT? Such circuits with the right continuum limit certainly exist, as we saw with the Shift circuit, introduced in section III D.

Here we have focused on the dynamics, but there are other key aspects of simulation, such as initial state preparation and measurement. Since the circuits here approximate the dynamics of QFTs, it should be sufficient to use any approximation of the ground or initial state of the QFT for simulations, as long as both the circuit dynamics and the initial state tend to their continuum counterparts in the continuum limit. For simulating scattering processes in ϕ^4 theory, state preparation and measurement were dealt with in [9]. And there are other details that cannot be swept under the rug, such as rates of convergence, as they affect the computational complexity of simulations. One way to deal with this is to use effective field theory to estimate the error arising from the discretization, as in [9], or to rely on results from Euclidean lattice QFT quantifying discretization errors and improving the action to reduce errors.

To conclude, let us mention one final point regarding renormalization for the circuits we have discussed or other quantum simulations of QFT. In practice, it would be interesting to do the renormalization via gradient descent, especially in cases where perturbative methods no longer work. This could work as follows. Physical parameters at a fixed energy scale are defined by certain processes, e.g., λ_{phys} can be defined by the amplitude for a specific process of two particles scattering to two particles, giving $-i\lambda_{\text{phys}}$ [43]. Now, suppose we know the values of all physical parameters g_{phys}^i at a given energy scale, which may come from some experiments. Then for our simulator at a fixed lattice spacing, to find the right bare parameters g_0^i , we simulate the scattering events (or other processes) that define the physical parameters giving some values $g_{\text{sim}}^i(g_0^j)$, which are functions of the bare parameters g_0^i . For ϕ^4 theory, these would be λ , m and the field-strength renormalization Z . Our goal is to change the bare parameters to minimize

$C = \sum_i [g_{\text{phys}}^i - g_{\text{sim}}^i(g_0^j)]^2$. To do this, we can approximate the derivatives of C with respect to g_0^i by also running the simulations with slightly shifted parameters $g_0^i + \delta g_0^i$. Then, based on this and following the usual recipe for gradient descent, we update our bare parameters: $g_0^i \rightarrow g_0^i - \eta \partial C / \partial g_0^i$, where $\eta > 0$ is a free parameter we would have to choose empirically. Or course, this comes with all the fineprint associated with gradient descent including the possibility of getting stuck in local minima. Nevertheless, even if the procedure is computationally expensive (we have no obvious guide to the computational complexity), it is a one-time cost: the best values of the bare parameters for a given lattice spacing need only be found once.

Note added

Close to completion of this work, a preprint [46] was posted on the arxiv that also looks at scattering in discrete-time models, the same topic discussed in section IV. In [46], discrete-time scattering methods were applied to a discretization of the Thirring model, which consists of fermions in one dimension interacting via a quartic interaction.

Acknowledgments

TCF was supported by the Australian Research Council Centres of Excellence for Engineered Quantum Systems (EQUS, CE170100009). The authors would like to thank Tobias Osborne and Dmytro Bondarenko for helpful discussions.

-
- [1] K. G. Wilson. Confinement of quarks. *Phys. Rev. D*, 10:2445–2459, 1974.
 - [2] M. Creutz. *Quarks, Gluons and Lattices*. Cambridge Monographs on Mathematical Physics. Cambridge University Press, 1983.
 - [3] T. DeGrand and C. DeTar. *Lattice Methods for Quantum Chromodynamics*. World Scientific, 2006.
 - [4] A. Maas. Lattice quantum field theory. Lecture notes at <https://physik.uni-graz.at/~axm/lattice2017.pdf>, 2017.
 - [5] S. Dürr, Z. Fodor, J. Frison, C. Hoelbling, R. Hoffmann, S. D. Katz, S. Krieg, T. Kurth, L. Lellouch, T. Lippert, K. K. Szabo, and G. Vulvert. Ab initio determination of light hadron masses. *Science*, 322(5905):1224–1227, 2008.
 - [6] M. Creutz. Confinement and the critical dimensionality of space-time. *Phys. Rev. Lett.*, 43:553–556, 1979.
 - [7] T. Appelquist, G. T. Fleming, and E. T. Neil. Lattice study of the conformal window in qcd-like theories. *Phys. Rev. Lett.*, 100:171607, 2008.
 - [8] T. Byrnes and Y. Yamamoto. Simulating lattice gauge theories on a quantum computer. *Phys. Rev. A*, 73:022328, 2006.
 - [9] S. P. Jordan, K. S. M. Lee, and J. Preskill. Quantum algorithms for quantum field theories. *Science*, 336(6085):1130–1133, 2012.
 - [10] S. P. Jordan, K. S. M. Lee, and J. Preskill. Quantum computation of scattering in scalar quantum field theories. *Quantum Information & Computation*, 14(11-12):1014–1080, 2014.
 - [11] S. P. Jordan, K. S. M. Lee, and J. Preskill. Quantum Algorithms for Fermionic Quantum Field Theories. arXiv:1404.7115, 2014.
 - [12] G. K. Brennen, P. Rohde, B. C. Sanders, and S. Singh. Multiscale quantum simulation of quantum field theory using wavelets. *Phys. Rev. A*, 92:032315, 2015.
 - [13] K. Marshall, R. Pooser, G. Siopsis, and C. Weedbrook. Quantum simulation of quantum field theory using continuous variables. *Phys. Rev. A*, 92:063825, 2015.
 - [14] S. P. Jordan, H. Krovi, K. S. M. Lee, and J. Preskill.

- BQP-completeness of scattering in scalar quantum field theory. *Quantum*, 2:44, 2018.
- [15] A. Alexandru, P. F. Bedaque, H. Lamm, and S. Lawrence. σ models on quantum computers. *Phys. Rev. Lett.*, 123:090501, 2019.
- [16] A. H. Moosavian, J. R. Garrison, and S. P. Jordan. Site-by-site quantum state preparation algorithm for preparing vacua of fermionic lattice field theories. arXiv:1911.03505, 2019.
- [17] C. Muschik, M. Heyl, E. Martinez, T. Monz, P. Schindler, B. Vogell, M. Dalmonte, P. Hauke, R. Blatt, and P. Zoller. U(1) wilson lattice gauge theories in digital quantum simulators. *New Journal of Physics*, 19(10):103020, 2017.
- [18] K. Yeter-Aydeniz, E. F. Dumitrescu, A. J. McCaskey, R. S. Bennink, R. C. Pooser, and G. Siopsis. Scalar quantum field theories as a benchmark for near-term quantum computers. *Phys. Rev. A*, 99:032306, 2019.
- [19] J. Preskill. Simulating quantum field theory with a quantum computer. arXiv:1811.10085, 2018.
- [20] E. A. Martinez, C. A. Muschik, P. Schindler, D. Nigg, A. Erhard, M. Heyl, P. Hauke, M. Dalmonte, T. Monz, P. Zoller, and R. Blatt. Real-time dynamics of lattice gauge theories with a few-qubit quantum computer. *Nature*, 534:516–516, 2016.
- [21] M. C. Bañuls, R. Blatt, J. Catani, A. Celi, J. I. Cirac, M. Dalmonte, L. Fallani, K. Jansen, M. Lewenstein, S. Montangero, C. A. Muschik, B. Reznik, E. Rico, L. Tagliacozzo, K. Van Acoleyen, F. Verstraete, U.-J. Wiese, M. Wingate, J. Zakrzewski, and P. Zoller. Simulating lattice gauge theories within quantum technologies. arXiv:1911.00003, 2019.
- [22] K. Wilson. The renormalization group and critical phenomena. In *Nobel Lectures, Physics 1981-1990*. World Scientific, 1993.
- [23] C. Muschik, M. Heyl, E. Martinez, T. Monz, P. Schindler, B. Vogell, M. Dalmonte, P. Hauke, R. Blatt, and P. Zoller. U(1) wilson lattice gauge theories in digital quantum simulators. *New Journal of Physics*, 19(10):103020, 2017.
- [24] T. Farrelly. A review of quantum cellular automata. arXiv:1904.13318, 2019.
- [25] P. Arrighi. An overview of quantum cellular automata. *Natural Computing*, 2019. <https://doi.org/10.1007/s11047-019-09762-6>.
- [26] T. C. Farrelly. *Insights from Quantum Information into Fundamental Physics*. PhD thesis, University of Cambridge, 2015. arXiv:1708.08897.
- [27] A. Bisio, G. M. D’Ariano, and A. Tosini. Quantum field as a quantum cellular automaton: the Dirac free evolution in one dimension. *Annals of Physics*, 354:244–264, 2015.
- [28] A. Bisio, G. M. D’Ariano, and P. Perinotti. Quantum cellular automaton theory of light. *Annals of Physics*, 368:177–190, 2016.
- [29] A. Bisio, G. M. D’Ariano, P. Perinotti, and A. Tosini. Weyl, Dirac and Maxwell quantum cellular automata. *Foundations of Physics*, 45(10):1203–1221, 2015.
- [30] G. M. D’Ariano and P. Perinotti. Quantum cellular automata and free quantum field theory. *Frontiers of Physics*, 45(10):1137–1152, 2017.
- [31] A. Bisio, G. M. D’Ariano, P. Perinotti, and A. Tosini. Free quantum field theory from quantum cellular automata: derivation of Weyl, Dirac and Maxwell quantum cellular automata. *Foundations of Physics*, 45(10):1137–1152, 2015.
- [32] C. Destri and H. J. de Vega. Light cone lattice approach to fermionic theories in 2-d: the massive Thirring model. *Nucl. Phys.*, B290:363, 1987.
- [33] A. Bisio, G. M. D’Ariano, P. Perinotti, and A. Tosini. Thirring quantum cellular automaton. *Phys. Rev. A*, 97:032132, 2018.
- [34] P. Arrighi, C. Bény, and T. Farrelly. A quantum cellular automaton for one-dimensional QED. *Quantum Information Processing*, 19:88, 2020.
- [35] J. Yepez. Quantum computational representation of gauge field theory. arXiv:1612.09291, 2016.
- [36] J. Yepez. Quantum lattice gas algorithmic representation of gauge field theory. *Proceedings, Quantum Information Science and Technology II*, 9996:99960N, 2016.
- [37] H. B. Nielsen and M. Ninomiya. A no-go theorem for regularizing chiral fermions. *Physics Letters B*, 105(2–3):219 – 223, 1981.
- [38] N. Klco and M. J. Savage. Digitization of scalar fields for quantum computing. *Phys. Rev. A*, 99:052335, 2019.
- [39] J. Kogut and L. Susskind. Hamiltonian formulation of Wilson’s lattice gauge theories. *Phys. Rev. D*, 11:395–408, 1975.
- [40] K. Marshall, R. Pooser, G. Siopsis, and C. Weedbrook. Repeat-until-success cubic phase gate for universal continuous-variable quantum computation. *Phys. Rev. A*, 91:032321, 2015.
- [41] M. Suzuki. Fractal decomposition of exponential operators with applications to many-body theories and Monte Carlo simulations. *Physics Letters A*, 146(6):319 – 323, 1990.
- [42] J. Smit. *Introduction to Quantum Fields on a Lattice*. Cambridge Lecture Notes in Physics. Cambridge University Press, 2002.
- [43] M. E. Peskin and D. V. Schroeder. *An Introduction to Quantum Field Theory*. Perseus Books Publishing, 1995.
- [44] D. Tong. Quantum field theory. Lecture notes at <http://www.damtp.cam.ac.uk/user/tong/qft.html>, 2006.
- [45] M. Gell-Mann and F. Low. Bound states in quantum field theory. *Phys. Rev.*, 84:350–354, 1951.
- [46] A. Bisio, N. Mosco, and P. Perinotti. Scattering and perturbation theory for discrete-time dynamics. arXiv:1912.09768, 2019.
- [47] Complete elliptic integral of the first kind: introduction to the complete elliptic integrals. <http://functions.wolfram.com/EllipticIntegrals/EllipticK/introductions/CompleteEllipticIntegrals/05/>. Accessed: 2019-12-06.

Appendix A: Scalar field theory

There are two approaches to deal with dynamics in QFT: path integrals or Hamiltonians. In this section, we will focus on the latter, so that dynamics are then generated by a local Hamiltonian H .

Let us recap the basics of scalar field theory in $D = (d + 1)$ dimensional continuous spacetime. For a good introduction, see, e.g., [43, 44]. In the Schrödinger picture, we can describe the system by starting with the

field operators $\phi(\mathbf{x})$ and $\pi(\mathbf{x})$ that live at each spatial point $\mathbf{x} \in \mathbb{R}^d$. The field operators obey the commutation relations

$$[\phi(\mathbf{x}), \pi(\mathbf{y})] = i\delta^{(d)}(\mathbf{x} - \mathbf{y}), \quad (\text{A1})$$

and $[\phi(\mathbf{x}), \phi(\mathbf{y})] = [\pi(\mathbf{x}), \pi(\mathbf{y})] = 0$. Then for a free scalar field the Hamiltonian has the form

$$H_0 = \frac{1}{2} \int d^d x [\pi^2(\mathbf{x}) + (\nabla\phi)^2(\mathbf{x}) + m^2\phi^2(\mathbf{x})], \quad (\text{A2})$$

where we are using units with $c = \hbar = 1$. To solve this, we make the ansatz that the field operators can be written as

$$\begin{aligned} \phi(\mathbf{x}) &= \int_{-\infty}^{\infty} \frac{d^d p}{2\pi} \frac{1}{\sqrt{2E(\mathbf{p})}} e^{i\mathbf{p}\cdot\mathbf{x}} (a_{\mathbf{p}} + a_{-\mathbf{p}}^\dagger) \\ \pi(\mathbf{x}) &= \int_{-\infty}^{\infty} \frac{d^d p}{2\pi} (-i) \sqrt{\frac{E(\mathbf{p})}{2}} e^{i\mathbf{p}\cdot\mathbf{x}} (a_{\mathbf{p}} - a_{-\mathbf{p}}^\dagger), \end{aligned} \quad (\text{A3})$$

where

$$E(\mathbf{p}) = \sqrt{\mathbf{p}^2 + m^2}, \quad (\text{A4})$$

and the bosonic creation and annihilation operators $a_{\mathbf{p}}^\dagger$ and $a_{\mathbf{p}}$ satisfy

$$\begin{aligned} [a_{\mathbf{q}}, a_{\mathbf{p}}^\dagger] &= 2\pi\delta^{(d)}(\mathbf{p} - \mathbf{q}) \\ [a_{\mathbf{q}}, a_{\mathbf{p}}] &= 0. \end{aligned} \quad (\text{A5})$$

These operators describe the free particles (excitations) of the field. Then the Hamiltonian has the simple form

$$H_0 = \int \frac{d^d p}{2\pi} E(\mathbf{p}) a_{\mathbf{p}}^\dagger a_{\mathbf{p}} + E_0. \quad (\text{A6})$$

Here $E(\mathbf{p})$ is understood as the energy of a particle with momentum \mathbf{p} . The ground state $|0\rangle$ is the state with no particles, so $|0\rangle$ is annihilated by all $a_{\mathbf{p}}$.

In the Heisenberg picture, operators evolve like

$$A(t, \mathbf{x}) = e^{iH_0 t} A(0, \mathbf{x}) e^{-iH_0 t}. \quad (\text{A7})$$

The equations of motion for field operators in the Heisenberg picture are

$$\begin{aligned} \partial_t \phi(x) &= \pi(x) \\ \partial_t \pi(x) &= (\nabla^2 - m^2)\phi(x), \end{aligned} \quad (\text{A8})$$

where $x = (t, \mathbf{x})$. Field operators take a nice form in the Heisenberg picture:

$$\phi(x) = \int_{-\infty}^{\infty} \frac{d^d p}{2\pi} \frac{1}{\sqrt{2E(\mathbf{p})}} (e^{-ip_s \cdot x} a_{\mathbf{p}} + e^{ip_s \cdot x} a_{\mathbf{p}}^\dagger), \quad (\text{A9})$$

where $p_s = (E(\mathbf{p}), \mathbf{p})$, where the subscript s indicates that we mean on-shell. Then $p_s \cdot x = E(\mathbf{p})t - \mathbf{p}\cdot\mathbf{x}$, so our convention for the metric is $\eta_{00} = 1$, $\eta_{ii} = -1$ where

$i \in \{1, \dots, d\}$ label spatial directions and $\eta_{\mu\nu} = 0$ if $\mu \neq \nu$. The Feynman propagator is given by

$$\begin{aligned} D_F(x-y) &= \langle 0 | \mathcal{T} [\phi(x)\phi(y)] | 0 \rangle \\ &= \int \frac{d^D p}{(2\pi)^D} \frac{i e^{-ip \cdot (x-y)}}{p^2 - m^2 + i\epsilon}, \end{aligned} \quad (\text{A10})$$

where the $i\epsilon$ term is necessary for the second equality to hold, but its limit to zero should be taken after any calculations. Here $D = d + 1$ is the dimension of spacetime.

To include an interaction, we add a term H_{int} to the Hamiltonian. The example we are interested in has interaction term:

$$H_{int} = \frac{\lambda}{4!} \int d^d x \phi^4(\mathbf{x}). \quad (\text{A11})$$

Appendix B: Relation of the Strang-split circuit to the path integral

Let us start by introducing a basis describing the field configurations on the lattice at time η such that

$$X_{\mathbf{n}} |x(\eta)\rangle = x_{\mathbf{n}}(\eta) |x(\eta)\rangle, \quad (\text{B1})$$

so here $x_{\mathbf{n}}(\eta)$ is a scalar, so we are using upper case letters for operators and lower case letters for scalars. Note also that $X_{\mathbf{n}}$ is proportional to $\phi_{\mathbf{n}}$, so these states are also eigenstates of the field operators $\phi_{\mathbf{n}}$. Furthermore, we have

$$\begin{aligned} |x(\eta)\rangle &= \prod_{\mathbf{n}} |x_{\mathbf{n}}(\eta)\rangle \\ \mathbb{1} &= \int dx(\eta) |x(\eta)\rangle \langle x(\eta)|, \end{aligned} \quad (\text{B2})$$

where $\int dx(\eta) = \int \prod_{\mathbf{n}} dx_{\mathbf{n}}(\eta)$. Note that if the spatial lattice is finite, then everything here is mathematically well defined. If the lattice is however infinite, i.e., \mathbb{Z}^d , then these expressions are only formal.

We have the initial and final field configurations $|x(0)\rangle$ and $|x(\tau)\rangle$ at time 0 and time τ respectively. The amplitude for one to evolve into the other is

$$\langle x(\tau) | U^\tau | x(0) \rangle = \langle x_\tau | (W_X W_P W_X)^\tau | x(0) \rangle, \quad (\text{B3})$$

where we have

$$\begin{aligned} W_P &= \prod_{\mathbf{n} \in \mathbb{Z}^d} \exp\left[\frac{-i\kappa}{2} P_{\mathbf{n}}^2\right] \\ W_X &= \prod_{\mathbf{n} \in \mathbb{Z}} \exp\left[\frac{-i\kappa}{2} V(X_{\mathbf{n}})\right], \end{aligned} \quad (\text{B4})$$

where

$$V(X_{\mathbf{n}}) = (d + \mu^2/2) X_{\mathbf{n}}^2 - \sum_{\mathbf{e} \in \mathcal{N}} X_{\mathbf{n}+\mathbf{e}} X_{\mathbf{n}} + \frac{\Lambda}{4!} X_{\mathbf{n}}^4. \quad (\text{B5})$$

Inserting factors of $\mathbb{1} = \int dx(\eta)|x(\eta)\rangle\langle x(\eta)|$, we get

$$\langle x(\tau)|U^\tau|x(0)\rangle = \int \prod_{\eta=1}^{\tau-1} dx(\eta) \prod_{\nu=0}^{\tau-1} \langle x(\nu+1)|W_X W_P W_X|x(\nu)\rangle. \quad (\text{B6})$$

We can simplify this via

$$\begin{aligned} & \langle x(\nu+1)|W_X W_P W_X|x(\nu)\rangle \\ &= \langle x(\nu+1)|W_P|x(\nu)\rangle e^{-i\frac{\kappa}{2} \sum_{\mathbf{n}} [V[x_{\mathbf{n}}(\nu+1)] + V[x_{\mathbf{n}}(\nu)]]}, \end{aligned} \quad (\text{B7})$$

where now $V[x_{\mathbf{n}}(\nu)]$ is a function of the scalars $x_{\mathbf{n}}(\nu)$. Also, we have

$$\langle x(\nu+1)|W_P|x(\nu)\rangle = \prod_{\mathbf{n}} \langle x_{\mathbf{n}}(\nu+1)|e^{-\frac{i\kappa}{2} P_{\mathbf{n}}^2}|x_{\mathbf{n}}(\nu)\rangle \quad (\text{B8})$$

Since $P_{\mathbf{n}}$ is the canonically conjugate variable to $X_{\mathbf{n}}$, we can insert the identity in the form of an integral over eigenvectors of $P_{\mathbf{n}}$, given by (dropping the \mathbf{n} indices for now)

$$\mathbb{1} = \int \frac{dp}{2\pi} |p\rangle\langle p|, \quad (\text{B9})$$

where the integral is over \mathbb{R} and

$$|p\rangle = \int \frac{dz}{2\pi} e^{ipz} |z\rangle. \quad (\text{B10})$$

Then we get

$$\begin{aligned} \langle y|e^{-\frac{i\kappa}{2} P^2}|z\rangle &= \int \frac{dp}{2\pi} \langle y|p\rangle\langle p|z\rangle e^{-\frac{i\kappa}{2} p^2} \\ &= \int \frac{dp}{2\pi} \exp\left(\frac{-i\kappa}{2} p^2 + ip(y-z)\right) \\ &= \sqrt{\frac{i}{2\pi\kappa}} \exp\left(\frac{i}{2\kappa} [y-z]^2\right). \end{aligned} \quad (\text{B11})$$

Putting this together, we get that

$$\langle x_\tau|U^\tau|x_0\rangle = \int D[x] \exp\left(i \sum_{\eta=0}^{\tau-1} \sum_{\mathbf{n}} L(\eta, \mathbf{n})\right) \quad (\text{B12})$$

where

$$\begin{aligned} L(\eta, \mathbf{n}) &= \frac{1}{2\kappa} [x_{\mathbf{n}}(\eta+1) - x_{\mathbf{n}}(\eta)]^2 \\ &\quad - \frac{\kappa}{2} [V[x_{\mathbf{n}}(\eta+1)] + V[x_{\mathbf{n}}(\eta)]] \end{aligned} \quad (\text{B13})$$

and

$$D[x] = \prod_{\nu=1}^{\tau-1} \left(\prod_{\mathbf{n}} dx_{\mathbf{n}}(\nu) \right) \left(\prod_{\mu=1}^{\tau-1} \prod_{\mathbf{m}} \sqrt{\frac{i}{2\pi\kappa}} \right). \quad (\text{B14})$$

Subbing in $x_{\mathbf{n}}(\nu) = a^{(d-1)/2} \varphi_{\nu, \mathbf{n}}$, we finally we see that

$$\langle \varphi_{\mathbf{f}}|U^\tau|\varphi_{\mathbf{i}}\rangle = \int \mathcal{D}(\varphi) e^{iS(\varphi)}, \quad (\text{B15})$$

where the action $S(\varphi)$ is given by

$$S(\varphi) = \sum_{\nu=0}^{\tau-1} \delta t \sum_{\mathbf{n}} a^d \mathcal{L}(\nu, \mathbf{n}), \quad (\text{B16})$$

with

$$\mathcal{L}(\nu, \mathbf{n}) = \frac{(\varphi_{\tau+1, \mathbf{n}} - \varphi_{\tau, \mathbf{n}})^2}{2\delta t^2} - \frac{\mathcal{V}(\varphi_{\nu, \mathbf{n}}) + \mathcal{V}(\varphi_{\nu, \mathbf{n}})}{2}. \quad (\text{B17})$$

$$\mathcal{V}(\varphi_{\nu, \mathbf{n}}) = \frac{1}{2} (\nabla_a \varphi_{\nu, \mathbf{n}})^2 + \frac{m^2}{2} \varphi_{\nu, \mathbf{n}}^2 + \frac{\lambda}{4!} \varphi_{\nu, \mathbf{n}}^4. \quad (\text{B18})$$

Finally, the measure is given by

$$\mathcal{D}(\varphi) = \prod_{\eta=1}^{\tau-1} \prod_{\mathbf{n}} \left(\sqrt{\frac{ia^{d-1}}{2\pi\kappa}} d\varphi_{\eta, \mathbf{n}} \right). \quad (\text{B19})$$

Appendix C: Solving the free QFT circuit

The evolution of the field over one timestep is given by

$$\begin{aligned} U_0^\dagger \phi(\mathbf{p}) U_0 &= c(\mathbf{p}) \phi(\mathbf{p}) + \delta t \pi(\mathbf{p}) \\ U_0^\dagger \pi(\mathbf{p}) U_0 &= c(\mathbf{p}) \pi(\mathbf{p}) + \frac{[c(\mathbf{p})^2 - 1]}{\delta t} \phi(\mathbf{p}), \end{aligned} \quad (\text{C1})$$

where

$$c(\mathbf{p}) = 1 + \kappa^2 \left[\sum_{i=1}^d \cos(p_i a) - d - \mu^2/2 \right]. \quad (\text{C2})$$

Other circuits, e.g., that given in appendix III D, can also be solved using the same methods, as they evolve the fields just as in equation (C1) only with a different $c(\mathbf{p})$ function.

To solve equation (C1), we need to find the annihilation operator

$$b_{\mathbf{p}} = \alpha(\mathbf{p}) \phi(\mathbf{p}) + \beta(\mathbf{p}) \pi(\mathbf{p}) \quad (\text{C3})$$

satisfying

$$U_0^\dagger b_{\mathbf{p}} U_0 = e^{-i\theta(\mathbf{p})\delta t} b_{\mathbf{p}}, \quad (\text{C4})$$

while also obeying

$$[b_{\mathbf{p}}, b_{\mathbf{q}}^\dagger] = (2\pi)^d \delta^{(d)}(\mathbf{p} - \mathbf{q}). \quad (\text{C5})$$

So our goal is to find $\alpha(\mathbf{p})$, $\beta(\mathbf{p})$ and $\theta(\mathbf{p})$. The most straightforward way to do this is to write equation (C4) as a matrix equation. To do this, we note that the dynamics of the field in equation (C1) can be specified by the matrix

$$\begin{pmatrix} c(\mathbf{p}) & \frac{c(\mathbf{p})^2 - 1}{\delta t} \\ \delta t & c(\mathbf{p}) \end{pmatrix}, \quad (\text{C6})$$

where the vector $(1, 0)^T$ represents $\phi(\mathbf{p})$ and $(0, 1)^T$ represents $\pi(\mathbf{p})$. This is symmetric under $\mathbf{p} \rightarrow -\mathbf{p}$. In matrix form, equation (C4) becomes the eigenvalue equation

$$\begin{pmatrix} c(\mathbf{p}) & \frac{c(\mathbf{p})^2 - 1}{\delta t} \\ \delta t & c(\mathbf{p}) \end{pmatrix} \begin{pmatrix} \alpha(\mathbf{p}) \\ \beta(\mathbf{p}) \end{pmatrix} = e^{-i\theta(\mathbf{p})\delta t} \begin{pmatrix} \alpha(\mathbf{p}) \\ \beta(\mathbf{p}) \end{pmatrix}. \quad (\text{C7})$$

(The other eigenvalue $e^{i\theta(\mathbf{p})\delta t}$ turns out to correspond to the creation operator $b_{\mathbf{p}}^\dagger$.) In order to get real solutions for $\theta(\mathbf{p})$ (which is the circuit's analogue of energy), we need to ensure that $-1 < c(\mathbf{p}) < 1$. This constraint follows because the trace of the matrix is $2c(\mathbf{p})$ which equals the sum of the eigenvalues, i.e., $2\cos[\theta(\mathbf{p})\delta t]$. We will go a little further and demand that $0 < c(\mathbf{p}) < 1$. This imposes a constraint on κ , which is

$$\kappa^2 < \frac{2}{4d + \mu^2}. \quad (\text{C8})$$

As an aside, the weaker constraint, that $-1 < c(\mathbf{p}) < 1$, allows circuits where $\theta(\mathbf{p})\delta t \sim \pi$ for some values of \mathbf{p} , which in some cases leads to a bosonic analogue of fermion doubling [37], where the equal-time propagator has large contributions from not only low momentum particles, but also high momentum particles. An example of this is given in section III D. It seems that the most general constraint that would work and rule out doubling would be $-K < c(\mathbf{p}) < 1$, with $K < 1$ and K independent of a . For simplicity, we will stick with $K = 0$.

Solving equation (C7) gives us

$$e^{-i\theta(\mathbf{p})\delta t} = c(\mathbf{p}) \pm \sqrt{c(\mathbf{p})^2 - 1}. \quad (\text{C9})$$

Since we know that $0 < c(\mathbf{p}) < 1$, we can rewrite this as

$$e^{-i\theta(\mathbf{p})\delta t} = c(\mathbf{p}) - i\sqrt{1 - c(\mathbf{p})^2}, \quad (\text{C10})$$

where the choice of the minus sign corresponds to positive $\theta(\mathbf{p})$. The other eigenvalue $e^{i\theta(\mathbf{p})\delta t}$, which has a plus sign, corresponds to the eigenvector $(\alpha^*(\mathbf{p}), \beta^*(\mathbf{p}))^T$, which describes the creation operator $b_{-\mathbf{p}}^\dagger$.

The eigenvalue equation does not fix $\alpha(\mathbf{p})$ and $\beta(\mathbf{p})$ uniquely. But we also have the constraint that $[b_{\mathbf{p}}, b_{\mathbf{q}}^\dagger] = (2\pi)^d \delta^{(d)}(\mathbf{p} - \mathbf{q})$, which implies that

$$\alpha(\mathbf{p})\beta^*(\mathbf{p}) - \alpha^*(\mathbf{p})\beta(\mathbf{p}) = -i. \quad (\text{C11})$$

Then we can satisfy this by choosing

$$\begin{aligned} \alpha(\mathbf{p}) &= \sqrt{\frac{\sin[\theta(\mathbf{p})\delta t]}{2\delta t}} \\ \beta(\mathbf{p}) &= i\sqrt{\frac{\delta t}{2\sin[\theta(\mathbf{p})\delta t]}}, \end{aligned} \quad (\text{C12})$$

which also solve equation (C7).

Next we can invert for $b_{\mathbf{p}}$ to find the field operators. We have

$$\begin{aligned} b_{\mathbf{p}}^\dagger &= \alpha^*(\mathbf{p})\phi^\dagger(\mathbf{p}) + \beta^*(\mathbf{p})\pi^\dagger(\mathbf{p}) \\ &= \alpha^*(\mathbf{p})\phi(-\mathbf{p}) + \beta^*(\mathbf{p})\pi(-\mathbf{p}), \end{aligned} \quad (\text{C13})$$

where we used that, e.g., $\phi^\dagger(\mathbf{p}) = \phi(-\mathbf{p})$. Also, noting that both $\alpha(\mathbf{p})$ and $\beta(\mathbf{p})$ are symmetric under $\mathbf{p} \rightarrow -\mathbf{p}$, which follows because $\theta(\mathbf{p})$ is also symmetric, we get

$$b_{-\mathbf{p}}^\dagger = \alpha^*(\mathbf{p})\phi(\mathbf{p}) + \beta^*(\mathbf{p})\pi(\mathbf{p}) \quad (\text{C14})$$

The trick now is to use this equation as well as equation (C3) to isolate $\phi(\mathbf{p})$. So we get

$$\begin{aligned} \beta^*(\mathbf{p})b_{\mathbf{p}} - \beta(\mathbf{p})b_{-\mathbf{p}}^\dagger &= [\beta^*(\mathbf{p})\alpha(\mathbf{p}) - \beta(\mathbf{p})\alpha^*(\mathbf{p})]\phi(\mathbf{p}) \\ &= -i\phi(\mathbf{p}), \end{aligned} \quad (\text{C15})$$

where the last line followed from equation (C11). Substituting in $\beta(\mathbf{p}) = i(2\omega(\mathbf{p}))^{-1/2}$, we get

$$\phi(\mathbf{p}) = \frac{1}{\sqrt{2\omega(\mathbf{p})}} [b_{\mathbf{p}} + b_{-\mathbf{p}}^\dagger]. \quad (\text{C16})$$

Fourier transforming gives

$$\begin{aligned} \phi(\mathbf{x}) &= \int \frac{d^d p}{(2\pi)^d} \frac{e^{i\mathbf{p}\cdot\mathbf{x}}}{\sqrt{2\omega(\mathbf{p})}} [b_{\mathbf{p}} + b_{-\mathbf{p}}^\dagger] \\ &= \int \frac{d^d p}{(2\pi)^d} \frac{1}{\sqrt{2\omega(\mathbf{p})}} [e^{i\mathbf{p}\cdot\mathbf{x}} b_{\mathbf{p}} + e^{-i\mathbf{p}\cdot\mathbf{x}} b_{\mathbf{p}}^\dagger]. \end{aligned} \quad (\text{C17})$$

Finally, going to the Heisenberg picture, and using that

$$\begin{aligned} U_0^\dagger b_{\mathbf{p}} U_0 &= e^{-i\theta(\mathbf{p})\delta t} b_{\mathbf{p}} \\ U_0^\dagger b_{\mathbf{p}}^\dagger U_0 &= e^{i\theta(\mathbf{p})\delta t} b_{\mathbf{p}}^\dagger, \end{aligned} \quad (\text{C18})$$

gives

$$\phi(x) = \int \frac{d^d p}{(2\pi)^d} \frac{1}{\sqrt{2\omega(\mathbf{p})}} (e^{-ip_s \cdot x} b_{\mathbf{p}} + e^{ip_s \cdot x} b_{\mathbf{p}}^\dagger), \quad (\text{C19})$$

where $p_s = (\theta(\mathbf{p}), \mathbf{p})$. Similarly, we find an expression for $\pi(x)$, which is

$$\pi(x) = -i \int \frac{d^d p}{(2\pi)^d} \sqrt{\frac{\omega(\mathbf{p})}{2}} (e^{-ip_s \cdot x} b_{\mathbf{p}} - e^{ip_s \cdot x} b_{\mathbf{p}}^\dagger). \quad (\text{C20})$$

Appendix D: Feynman propagator

The Feynman propagator is defined to be

$$D_F(x - y) = \langle 0 | \mathcal{T}[\phi(x)\phi(y)] | 0 \rangle \quad (\text{D1})$$

where \mathcal{T} is the time-ordering operator. Inserting the formula for $\phi(x)$ from equation (C19), this becomes

$$D_F(x - y) = \begin{cases} \int \frac{d^d p}{(2\pi)^d} \frac{e^{-ip_s \cdot (x-y)}}{2\omega(\mathbf{p})} & x^0 > y^0 \\ \int \frac{d^d p}{(2\pi)^d} \frac{e^{ip_s \cdot (x-y)}}{2\omega(\mathbf{p})} & x^0 < y^0. \end{cases} \quad (\text{D2})$$

We can use the fact that both $\omega(\mathbf{p}) = \omega(-\mathbf{p})$ and $\theta(\mathbf{p}) = \theta(-\mathbf{p})$ to rewrite this as

$$\begin{aligned} D_F(x-y) &= \int \frac{d^d p}{(2\pi)^d} \frac{e^{i\mathbf{p}\cdot(\mathbf{x}-\mathbf{y})} e^{-i\theta(\mathbf{p})|x_0-y_0|}}{2\omega(\mathbf{p})} \\ &= \frac{\delta t}{2} \int \frac{d^d p}{(2\pi)^d} \frac{e^{i\mathbf{p}\cdot(\mathbf{x}-\mathbf{y})} e^{-i\theta(\mathbf{p})|x_0-y_0|}}{\sin[\theta(\mathbf{p})\delta t]}, \end{aligned} \quad (\text{D3})$$

where we used $\omega(\mathbf{p}) = \sin[\theta(\mathbf{p})\delta t]/\delta t$ to get the final line. To rewrite this in a nicer way, we will show below, via contour integration, that

$$\frac{e^{-i\theta_\varepsilon(\mathbf{p})|t|}}{\sin[\theta_\varepsilon(\mathbf{p})\delta t]} = \delta t \int_{-\pi/\delta t}^{\pi/\delta t} \frac{dp_0}{2\pi} \frac{ie^{-ip_0 t}}{\cos[\theta_\varepsilon(\mathbf{p})\delta t] - \cos(p_0\delta t)}, \quad (\text{D4})$$

where we have $\theta_\varepsilon(\mathbf{p}) = \theta(\mathbf{p}) - i\varepsilon$. Then we get that the propagator can be written as

$$D_F(x-y) = \frac{\delta t^2}{2} \int \frac{d^D p}{(2\pi)^D} \frac{ie^{-ip\cdot(x-y)}}{\cos[\theta_\varepsilon(\mathbf{p})\delta t] - \cos(p_0\delta t)}. \quad (\text{D5})$$

So we just need to do the contour integral to get equation (D4). This is equivalent to proving that

$$\begin{aligned} \frac{e^{-i(w-i\delta)|\tau|}}{\sin(w-i\delta)} &= \int_{-\pi}^{\pi} \frac{dz}{2\pi} \frac{ie^{-iz\tau}}{\cos(w-i\delta) - \cos(z)} \\ &= \int_{-\pi}^{\pi} dz f(z), \end{aligned} \quad (\text{D6})$$

where we used the substitutions $z = p_0\delta t$, $w = \theta(\mathbf{p})\delta t$, $\delta = \varepsilon\delta t$ and $\tau = t/\delta t$. Note that τ is an integer and $w \in (0, \pi)$. We can do the integral by contour integration using the contours shown in figure 4. The only poles are located at $z = \pm(w - i\delta)$. The residues at those points are given by

$$\begin{aligned} \text{Res}(f, w - i\delta) &= \frac{ie^{-i(w-i\delta)\tau}}{2\pi \sin(w - i\delta)} \\ \text{Res}(f, -w + i\delta) &= -\frac{ie^{i(w-i\delta)\tau}}{2\pi \sin(w - i\delta)}. \end{aligned} \quad (\text{D7})$$

Let us do the integral for the case with $\tau > 0$, which corresponds to the bottom contour \mathcal{B} in figure 4. Then

$$\begin{aligned} \int_{\mathcal{B}(\Lambda)} dz f(z) &= \sum_{i=1}^4 \int_{\mathcal{B}_i(\Lambda)} dz f(z) \\ &= \int_{\mathcal{B}_1(\Lambda)} dz f(z) + \int_{\mathcal{B}_3(\Lambda)} dz f(z), \end{aligned} \quad (\text{D8})$$

which follows because $f(\pi+i\lambda) = f(-\pi+i\lambda)$ ensures that the integral over $\mathcal{B}_2(\Lambda)$ cancels that over $\mathcal{B}_4(\Lambda)$. Then because of the choice of contour, we have that

$$\begin{aligned} \int_{\mathcal{B}_3(\Lambda)} dz f(z) &= \int_{\pi}^{-\pi} dp f(p - i\Lambda) \\ &= \int_{\pi}^{-\pi} \frac{dp}{2\pi} \frac{e^{-ip\tau} e^{-\Lambda\tau}}{\cos(w - i\delta) - \cos(p - i\Lambda)}, \end{aligned} \quad (\text{D9})$$

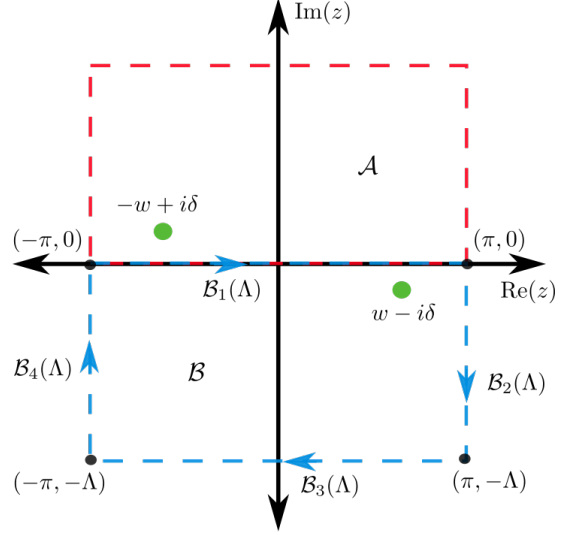


FIG. 4: Contour for the integral in equation (D6).

which goes to zero as $\Lambda \rightarrow \infty$ since $\tau > 0$. Then using Cauchy's integral formula, we have that

$$\begin{aligned} \int_{\mathcal{B}_1(\Lambda)} dz f(z) &= (-2\pi i) \frac{ie^{-i(w-i\delta)\tau}}{2\pi \sin(w - i\delta)}, \\ &= \frac{e^{-i(w-i\delta)\tau}}{\sin(w - i\delta)}. \end{aligned} \quad (\text{D10})$$

where the minus sign in the first line comes from the direction of the contour. For the integral with $\tau < 0$, which corresponds to the top contour \mathcal{A} , a similar argument shows that

$$\int_{\mathcal{B}_1(\Lambda)} dz f(z) = \frac{e^{i(w-i\delta)\tau}}{\sin(w - i\delta)}. \quad (\text{D11})$$

Appendix E: Deriving the Feynman rules

We want to calculate scattering amplitudes like

$$\langle f | S | i \rangle, \quad (\text{E1})$$

where $|i\rangle$ and $|f\rangle$ are initial and final states. For simplicity, let us focus on the case with two incoming and two outgoing particles, so we take

$$\begin{aligned} |i\rangle &= |\mathbf{p}_1 \mathbf{p}_2\rangle = \sqrt{2\omega(\mathbf{p}_1)} \sqrt{2\omega(\mathbf{p}_2)} b_{\mathbf{p}_1}^\dagger b_{\mathbf{p}_2}^\dagger |0\rangle \\ |f\rangle &= |\mathbf{k}_1 \mathbf{k}_2\rangle = \sqrt{2\omega(\mathbf{k}_1)} \sqrt{2\omega(\mathbf{k}_2)} b_{\mathbf{k}_1}^\dagger b_{\mathbf{k}_2}^\dagger |0\rangle. \end{aligned} \quad (\text{E2})$$

Next we insert

$$S = \mathcal{T} \left[\exp \left(-ia^d \delta t \frac{\lambda}{4!} \sum_x \phi(x)^4 \right) \right], \quad (\text{E3})$$

where \sum_x is shorthand for the sum over all spacetime points, i.e., $\sum_{\mathbf{n} \in \mathbb{Z}^d} \sum_{\tau \in \mathbb{Z}}$. Taylor expanding to order λ , we get

$$\langle f|S|i \rangle = \langle f|i \rangle - ia^d \delta t \frac{\lambda}{4!} \sum_x \langle f|\phi(x)^4|i \rangle + O(\lambda^2). \quad (\text{E4})$$

The zeroth order term is simply

$$\begin{aligned} \langle f|i \rangle &= 4\omega(\mathbf{p}_1)\omega(\mathbf{p}_2)(2\pi)^6 \left[\delta^d(\mathbf{p}_1 - \mathbf{k}_1)\delta^d(\mathbf{p}_2 - \mathbf{k}_2) \right. \\ &\quad \left. + \delta^d(\mathbf{p}_1 - \mathbf{k}_2)\delta^d(\mathbf{p}_2 - \mathbf{k}_1) \right], \end{aligned} \quad (\text{E5})$$

where $\delta^d(\mathbf{p}) = \delta_a(p_1)\dots\delta_a(p_d)$ with $\delta_a(q)$ denoting the lattice momentum delta function with period $2\pi/a$.

The zeroth order term is not so interesting, so we will focus on evaluating \mathcal{M} , defined by

$$\langle f|S - 1|i \rangle = (2\pi)^D \delta^D(p_1 + p_2 - k_1 - k_2) i\mathcal{M}, \quad (\text{E6})$$

where $\delta^D(p) = \delta_{\delta t}(p_0)\delta_a(p_1)\dots\delta_a(p_d)$. Here $\delta_a(q)$ denotes the lattice momentum delta function as before, and $\delta_{\delta t}(q)$ denotes the quasi-energy delta function with period $2\pi/\delta t$. Total energy and momentum will always be conserved, which is the reason we factor this delta function out in our definition of \mathcal{M} .

To evaluate the first order term (and the higher order terms), it will help to recall Wick's theorem (see, e.g., [43]). This states that

$$\mathcal{T}[\phi(x_1)\dots\phi(x_N)] = \mathcal{N}[\phi(x_1)\dots\phi(x_N) + \text{all contractions}]. \quad (\text{E7})$$

Here $\mathcal{N}[\cdot]$ denotes normal ordering of operators, which means that all creation operators are shifted to the left of all annihilation operators, e.g., $\mathcal{N}[b_{\mathbf{p}_1} b_{\mathbf{p}_2}^\dagger b_{\mathbf{p}_3}] = b_{\mathbf{p}_2}^\dagger b_{\mathbf{p}_1} b_{\mathbf{p}_3}$. Also, a contraction between two fields is defined to be

$$\overline{\phi(x)\phi(y)} = \langle \mathcal{T}[\phi(x)\phi(y)] \rangle = D_F(x - y). \quad (\text{E8})$$

Then the term ‘‘all contractions’’ means the sum of all possible contractions of $\phi(x_1)\dots\phi(x_N)$, e.g.,

$$\begin{aligned} \phi(x_1)\phi(x_2)\phi(x_3)\phi(x_4) &= \overline{\phi(x_1)\phi(x_2)\phi(x_3)\phi(x_4)} \\ &\quad + \overline{\phi(x_1)\phi(x_2)\phi(x_3)\phi(x_4)} \\ &\quad + \dots \end{aligned} \quad (\text{E9})$$

Operators that are contracted just contribute a Feynman propagator, whereas uncontracted field operators are cancelled by the creation and annihilation operators of the initial and final states. So we can define the contraction of a field operator with a creation operator to be

$$\overline{\phi_I(x)|\mathbf{p}} = \overline{\phi_I(x)\sqrt{2\omega(\mathbf{p})}b_{\mathbf{p}}^\dagger} = e^{-ip \cdot x}. \quad (\text{E10})$$

Then to calculate, e.g., the $O(\lambda)$ term, we evaluate all possible contractions of the fields and the initial and final state creation and annihilation operators. As an example contributing to the $O(\lambda)$ term, consider the contraction

$$\overline{\langle \mathbf{k}_1 \mathbf{k}_2 | \phi(x)\phi(x)\phi(x)\phi(x) | \mathbf{p}_1 \mathbf{p}_2 \rangle} = e^{-i(p_1+p_2-k_1-k_2) \cdot x}. \quad (\text{E11})$$

Then the overall contribution to $i\mathcal{M}$ from this contraction is

$$\begin{aligned} &-ia^d \delta t \frac{\lambda}{4!} \sum_x e^{-i(p_1+p_2-k_1-k_2) \cdot x} \\ &= -i \frac{\lambda}{4!} (2\pi)^D \delta^D(p_1 + p_2 - k_1 - k_2), \end{aligned} \quad (\text{E12})$$

where we used the identities $\sum_{n \in \mathbb{Z}} e^{inz} = 2\pi\delta(z)$ and $\delta(Cz) = \delta(z)/C$. We see the factors of $(2\pi)^D \delta^D(p_1 + p_2 - k_1 - k_2)$ as expected from our definition of \mathcal{M} . We assign the diagram in figure 5 to this contraction.

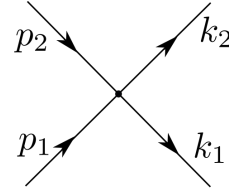


FIG. 5: A diagram contributing to the $O(\lambda)$ component of the scattering amplitude.

In fact, there are $4!$ possible contractions giving rise to the same diagram, which cancels the $1/4!$ factor in the interaction and simplifies the Feynman rules. The $1/4!$ factors do not always cancel for a given diagram, which is the reason for symmetry factors in the Feynman rules, as we will see.

A more interesting example comes from the order λ^2 contribution to the amplitude. Consider

$$\begin{aligned} &\overline{\langle \mathbf{k}_1 \mathbf{k}_2 | \phi(x)\phi(x)\phi(x)\phi(x)\phi(y)\phi(y)\phi(y)\phi(y) | \mathbf{p}_1 \mathbf{p}_2 \rangle} \\ &= e^{-i(p_1+p_2) \cdot x + i(k_1+k_2) \cdot y} D_F(x - y) D_F(x - y). \end{aligned} \quad (\text{E13})$$

The full contribution to the amplitude is then

$$\begin{aligned} &-a^{2d} \delta t^2 \frac{\lambda^2}{2(4!)^2} \sum_{x,y} e^{-i(p_1+p_2) \cdot x + i(k_1+k_2) \cdot y} D_F(x - y)^2 \\ &= \frac{-\lambda^2}{2(4!)^2} (2\pi)^{2D} \int \frac{d^D q_1 d^D q_2}{(2\pi)^{2D}} \delta^D(p_1 + p_2 - q_1 - q_2) \times \\ &\quad \times \delta^D(q_1 + q_2 - k_1 - k_2) D_F(q_1) D_F(q_2) \\ &= \frac{-\lambda^2}{2(4!)^2} (2\pi)^D \delta^D(p_1 + p_2 - k_1 - k_2) \times \\ &\quad \times \int \frac{d^D q}{(2\pi)^D} D_F(q) D_F(p_1 + p_2 - q), \end{aligned} \quad (\text{E14})$$

where the second line followed by plugging in the definition of the Feynman propagator:

$$\begin{aligned} D_F(x-y) &= \int \frac{d^D p}{(2\pi)^D} e^{-ip \cdot (x-y)} D_F(p) \\ &= \int \frac{d^D p}{(2\pi)^D} e^{ip \cdot (x-y)} D_F(p), \end{aligned} \quad (\text{E15})$$

where by abuse of notation $D_F(p)$ denotes the momentum space propagator, and we used that $D_F(p) = D_F(-p)$. The diagram corresponding to this process is given in figure 6. The number of contractions contribut-

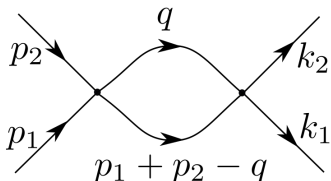


FIG. 6: A diagram contributing to the $O(\lambda^2)$ component of the scattering amplitude.

ing to this diagram is $(4!)^2$, which cancels the $1/(4!)^2$ factor and means that the symmetry factor is $1/2$, since a factor of $1/2$ came from the Taylor expansion of S . In practice, one finds the symmetry factor by looking at the symmetries of the diagram using the rules given in, e.g., [43], as opposed to counting the number of different contractions. The important point for us is that the symmetry factors for diagrams are the same as those in QFT.

This procedure of contracting fields by hand for terms in the expansion of S can be replaced by the Feynman rules. These rules (in momentum space) for calculating $i\mathcal{M}$ are as follows.

1. Draw all possible amputated and connected diagrams with the right number of incoming and outgoing legs.
2. Assign a directed momentum to each line, with energy and momentum conservation at each vertex.
3. Each internal line picks up a momentum-space propagator $D_F(p)$.
4. Each vertex gets a factor of $-i\lambda$.
5. Integrate over all undetermined momenta via

$$\int \frac{d^D p}{(2\pi)^D}.$$

6. Divide by the symmetry factor of each diagram.

We still have to justify the assumption of ‘‘amputated and connected’’ diagrams. First, ‘‘connected’’ means that every part of the diagram is connected to at least one

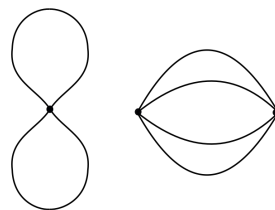


FIG. 7: A diagram describing vacuum bubbles that do not contribute to scattering amplitudes.

external leg. Basically, this excludes vacuum bubbles, meaning it rules out diagrams such as that in figure 7. One way to motivate this is to argue that the following formula, relating correlation functions in the interacting theory to calculations with the free vacuum, should hold:

$$\langle \Omega | \phi_H(x_1) \dots \phi_H(x_N) | \Omega \rangle = \frac{\langle 0 | \mathcal{T} [\phi(x_1) \dots \phi(x_N) S] | 0 \rangle}{\langle 0 | S | 0 \rangle}, \quad (\text{E16})$$

where $|\Omega\rangle$ is a state analogous to the vacuum in the presence of interactions and $\phi_H(x) = U^{-x_0/\delta t} \phi_{\mathbf{x}/a} U^{x_0/\delta t}$ denotes the field in the Heisenberg picture. The division by $\langle 0 | S | 0 \rangle$ on the right hand side is what cancels vacuum bubbles and justifies the restriction to connected diagrams.

Equation (E16) holds if we can make sense of

$$|\Omega\rangle \langle \Omega | 0 \rangle = \lim_{T \rightarrow \infty} U^T | 0 \rangle. \quad (\text{E17})$$

To see this, we assume for simplicity that $x_1^0 \geq x_2^0 \geq \dots \geq x_N^0$ to get

$$\begin{aligned} &\langle 0 | \mathcal{T} [\phi(x_1) \dots \phi(x_N) S] | 0 \rangle \\ &= \lim_{T \rightarrow \infty} \langle 0 | U(T, t_1) \phi(x_1) U(t_1, t_2) \phi(x_2) \dots U(t_N, -T) | 0 \rangle \\ &= \lim_{T \rightarrow \infty} \langle 0 | U^T \phi_H(x_1) \dots \phi_H(x_N) U^T | 0 \rangle. \end{aligned} \quad (\text{E18})$$

To get the second line, we use that the time-ordering operator splits up $S = \lim_{T \rightarrow \infty} U(T, -T)$ into each of the $U(t_i, t_j)$ terms, where we are abusing the notation a little to identify $U(t_i, t_j) = U(\tau_i, \tau_j)$, with $t_i = \tau_i \delta t$. The last line follows by using the definition of the field operators in the interaction picture, $\phi(x) = U_0^{\dagger x_0/t} \phi_{\mathbf{x}/a} U_0^{x_0/\delta t}$, and the definition of $U(t, 0) = U(\tau, 0) = U_0^{\dagger \tau} U^\tau$. It may be useful to note that $U(t_1, t_2) = U(t_1, 0) U(t_2, 0)^{-1}$.

We can give a rough justification for equation (E17), if the operator U has an eigenvector $|\Omega\rangle$ with eigenvalue 1 and the rest of its spectrum is continuous. Then, following [44], we can (very roughly) argue that, for any state $|\psi\rangle$,

$$\begin{aligned} &\lim_{T \rightarrow \infty} \langle \psi | U^T | 0 \rangle \\ &= \langle \psi | \Omega \rangle \langle \Omega | 0 \rangle + \lim_{T \rightarrow \infty} \int d\alpha e^{-i\alpha T} \langle \psi | \alpha \rangle \langle \alpha | 0 \rangle \\ &= \langle \psi | \Omega \rangle \langle \Omega | 0 \rangle, \end{aligned} \quad (\text{E19})$$

where $U|\alpha\rangle = e^{-i\alpha}|\alpha\rangle$ and α labels the continuous part of the spectrum. Getting the last line of equation (E19) is justified by the Riemann-Lebesgue lemma, which tells us that, for an L^1 function $f(x)$, $\int_{\mathbb{R}} dx f(x)e^{-ixz} \rightarrow 0$ as $|z| \rightarrow \infty$. In this case, we are assuming that $\langle\psi|\alpha\rangle\langle\alpha|0\rangle$ is an L^1 function of α . This is not a rigorous argument, which instead we postpone to future work.

Regarding ‘‘amputated’’ diagrams, this means that we do not include any diagrams with loops on external legs. Loops on external legs correspond to the fact that the propagator of the in-going and out-coming particles is modified in the interacting theory, which is motivated properly via the LSZ reduction theorem [43], which describes how to correctly relate S matrix elements to correlation functions. Again we postpone a thorough investigation of this to future work.

Appendix F: One-loop calculation

We want to evaluate the one-loop correction to the mass for different regulators. Let us consider the case of the Strang-split circuit first. This gives us

$$\Pi_{\text{Strang}}(p_{\text{in}}^2) = \frac{\lambda}{4} \int \frac{dp}{2\pi} \frac{\delta t}{\sqrt{1-c(p)^2}}, \quad (\text{F1})$$

where

$$c(p) = 1 + \kappa^2 [\cos(pa) - 1 - (ma)^2/2]. \quad (\text{F2})$$

At this point, we can introduce an arbitrary $m < \Delta \ll 1$ to break up the integral:

$$\Pi_{\text{Strang}}(p_{\text{in}}^2) = \frac{\lambda}{4\pi} \left(\int_0^{\Delta/a} \frac{\delta t dp}{\sqrt{1-c^2(p)}} + \int_{\Delta/a}^{\pi/a} \frac{\delta t dp}{\sqrt{1-c^2(p)}} \right). \quad (\text{F3})$$

Since we chose κ such that $0 < c(p) < 1$, the second term is positive and bounded above by

$$\frac{\kappa(\pi - \Delta)}{\sqrt{1 - (1 + \kappa^2 [\cos(\Delta) - 1])^2}}, \quad (\text{F4})$$

which is finite with no a dependence. Because $pa < \Delta \ll 1$, the first term in equation (F3) is well approximated by

$$\int_0^{\Delta/a} \frac{\delta t dp}{\sqrt{1-c^2(p)}} = \int_0^{\Delta/a} \frac{dp}{\sqrt{m^2 + p^2}} + \text{finite}. \quad (\text{F5})$$

The finite part can be approximated by finding the next order corrections to $1 - c^2(p) \simeq (m^2 + p^2)\delta t^2$. Putting

this all together, we have

$$\begin{aligned} \Pi_{\text{Strang}}(p_{\text{in}}^2) &= \frac{\lambda}{4\pi} \int_0^{\Delta/a} \frac{dp}{\sqrt{p^2 + m^2}} + \text{finite} \\ &= \frac{\lambda}{4\pi} \int_0^{\Delta/(ma)} \frac{dx}{\sqrt{x^2 + 1}} + \text{finite} \\ &= \frac{\lambda}{4\pi} \text{arcsinh} \left(\frac{\Delta}{ma} \right) + \text{finite} \\ &= \frac{\lambda}{4\pi} \ln \left(\frac{\Delta}{ma} \right) + \text{finite}. \end{aligned} \quad (\text{F6})$$

We can compare this to the same calculation from QFT with a momentum cutoff Λ , which is given by

$$\begin{aligned} \Pi_{\text{cont}}(p_{\text{in}}^2) &= -i\lambda \frac{1}{2} \int \frac{d^2 p}{(2\pi)^2} D_F^{\text{cont}}(p) \\ &= \frac{\lambda}{8\pi} \int_{-\Lambda}^{\Lambda} \frac{dp}{\sqrt{p^2 + m^2}} \\ &= \frac{\lambda}{4\pi} \ln \left(\frac{\Lambda}{m} \right) + \text{finite}, \end{aligned} \quad (\text{F7})$$

where $D_F^{\text{cont}}(p) = i/(p^2 + m^2)$ is the continuum propagator in momentum space. Again we see the logarithmic divergence with the cutoff.

Finally, we consider the Shift circuit. Using the naive Feynman rules, with the factor $-i\lambda$ assigned to each vertex, we have to evaluate

$$\Pi_{\text{shift}}(p_{\text{in}}^2) = \frac{\lambda}{4} \int \frac{dp}{2\pi} \frac{\delta t}{\sqrt{1-c(p)^2}}, \quad (\text{F8})$$

where we have a different $c(p)$ function given by

$$c(p) = M \cos(pa), \quad (\text{F9})$$

where $M = 1 - m^2 a^2 / 2$. We can evaluate this integral in terms of the complete elliptic integral of the first kind:

$$\begin{aligned} \Pi_{\text{shift}}(p_{\text{in}}^2) &= \frac{\lambda}{4} \int_{-\pi/a}^{\pi/a} \frac{dp}{2\pi} \frac{a}{\sqrt{1 - M^2 \cos(pa)^2}} \\ &= \frac{\lambda}{8\pi} \int_{-\pi}^{\pi} d\theta \frac{1}{\sqrt{1 - M^2 \cos(\theta)^2}} \\ &= \frac{\lambda}{2\pi} \int_0^{\pi/2} d\theta \frac{1}{\sqrt{1 - M^2 \sin(\theta)^2}} \\ &= \frac{\lambda}{2\pi} K(M), \end{aligned} \quad (\text{F10})$$

where $K(x)$ is the complete elliptic integral of the first kind. This can be expanded for $|x|$ close to one as [47]

$$K(x) = -\frac{1}{2} \ln(1 - x^2) + \text{const}. \quad (\text{F11})$$

Note that in the notation in [47], $K(x)$ is actually denoted

by $K(x^2)$. Plugging this in, we get

$$\begin{aligned}\Pi_{\text{shift}}(p_{\text{in}}^2) &= -\frac{\lambda}{4\pi} \ln(1 - M^2) + \text{finite} \\ &= -\frac{\lambda}{4\pi} \ln[m^2 a^2 + O(a^4)] + \text{finite} \quad (\text{F12}) \\ &= \frac{\lambda}{2\pi} \ln\left(\frac{1}{ma}\right) + \text{finite}.\end{aligned}$$

So we get a prefactor that is different from the other regulators by a factor of two. This can be traced back to the high-momentum modes with small values of $\omega(\mathbf{p})$ discussed in section III D. To remedy this, let us try instead using a modified interaction term:

$$V = a^D \frac{\lambda}{4!} \sum_{\mathbf{n} \in \mathbb{Z}^d} \left(\sum_{\mathbf{e} \in \mathcal{K}} w(\mathbf{e}) \phi_{\mathbf{n}+\mathbf{e}} \right)^4, \quad (\text{F13})$$

where \mathcal{K} is the set of all vectors with components in $\{-1, 0, 1\}$ and $w(\mathbf{e}) = v(e_1) \times \dots \times v(e_d)$ with $v(-1) = v(1) = 1/4$ and $v(0) = 1/2$. The weights $w(\mathbf{e})$ were chosen in order to have

$$\sum_{\mathbf{e} \in \mathcal{K}} w(\mathbf{e}) e^{i\mathbf{p} \cdot \mathbf{e} a} = \prod_{i=1}^d \frac{1 + \cos[p_i a]}{2}. \quad (\text{F14})$$

As a result of this, the Feynman rules are modified, with the sole change being that each vertex gets a factor of

$$-i\lambda \prod_{\chi=1}^4 \left[\prod_{i=1}^d \frac{1 + \cos[p_i^\chi a]}{2} \right], \quad (\text{F15})$$

where p_i^χ is the i th component of the momentum of the χ th line joining the vertex.

Now, the new integral for the one-loop diagram is

$$\begin{aligned}\Pi_{\text{shift}}(p_{\text{in}}^2) &= \frac{\lambda}{4} \frac{(1 + \cos[p_{\text{in}} a])^2}{16} \int \frac{d\mathbf{p}}{2\pi} \frac{a[1 + \cos(pa)]^2}{\sqrt{1 - M^2 \cos(pa)^2}}. \quad (\text{F16})\end{aligned}$$

Let us ignore the prefactor and focus on the integral for now:

$$\begin{aligned}& \int_{-\pi/a}^{\pi/a} \frac{d\mathbf{p}}{2\pi} \frac{a[1 + \cos(pa)]^2}{\sqrt{1 - M^2 \cos(pa)^2}} \\ &= \int_{-\pi}^{\pi} \frac{d\theta}{2\pi} \frac{[1 + \cos(\theta)]^2}{\sqrt{1 - M^2 \cos(\theta)^2}} \quad (\text{F17}) \\ &= \int_{-\pi}^{\pi} \frac{d\theta}{2\pi} \frac{1 + \cos(\theta)^2}{\sqrt{1 - M^2 \cos(\theta)^2}}.\end{aligned}$$

The last line follows because the integral vanishes for the terms with numerator linear in $\cos(\theta)$. To see this, use

$\cos(x) = -\cos(x + \pi)$. Then we get

$$\begin{aligned}& \int_{-\pi}^{\pi} \frac{d\theta}{2\pi} \left[\frac{1 + 1/M^2}{\sqrt{1 - M^2 \cos(\theta)^2}} + \frac{M^2 \cos(\theta)^2 - 1}{M^2 \sqrt{1 - M^2 \cos(\theta)^2}} \right] \\ &= \frac{2(1 + 1/M^2)K(M)}{\pi} - \int_{-\pi}^{\pi} \frac{d\theta}{2\pi} \frac{\sqrt{1 - M^2 \cos(\theta)^2}}{M^2} \\ &= \frac{2(1 + 1/M^2)K(M)}{\pi} + \text{finite}, \quad (\text{F18})\end{aligned}$$

where the last line follows from $0 \leq \sqrt{1 - M^2 \cos(\theta)^2} \leq 1$ and $M = 1 - m^2 a^2/2$, so $1/M^2 = 1 + O(a^2)$ for small a . Then we get

$$\int_{-\pi/a}^{\pi/a} \frac{d\mathbf{p}}{2\pi} \frac{a[1 + \cos(pa)]^2}{\sqrt{1 - M^2 \cos(pa)^2}} = \frac{4K(M)}{\pi} + \text{finite}. \quad (\text{F19})$$

This gives us

$$\Pi_{\text{shift}}(p_{\text{in}}^2) = \frac{(1 + \cos[p_{\text{in}} a])^2}{16} \frac{\lambda K(M)}{\pi} + \text{finite}. \quad (\text{F20})$$

Using the same expansion for the elliptic integral K as before, we get finally

$$\Pi_{\text{shift}}(p_{\text{in}}^2) = \frac{(1 + \cos[p_{\text{in}} a])^2}{4} \frac{\lambda}{4\pi} \ln\left(\frac{1}{ma}\right) + \text{finite}. \quad (\text{F21})$$

For small incoming momenta p_{in} compared to $1/a$, this agrees well with the calculations earlier of $\Pi_{\text{Strang}}(p_{\text{in}}^2)$ and $\Pi_{\text{cont}}(p_{\text{in}}^2)$ since $(1 + \cos[p_{\text{in}} a])^2 = 4 + O(a^2)$. For comparison, all of the functions $\Pi_{\text{Strang}}(p_{\text{in}}^2)$, $\Pi_{\text{cont}}(p_{\text{in}}^2)$ and $\Pi_{\text{shift}}(p_{\text{in}}^2)$ integrated numerically are plotted in figure 8 as a function of the lattice spacing a , where we take the momentum cutoff $\Lambda = \pi/a$ for comparison. Note that in the case of $\Pi_{\text{shift}}(p_{\text{in}}^2)$, we are considering the modified interaction term, so we are integrating equation (F16) numerically.

Appendix G: Non-abelian circuit and path integral

For a good description of how to connect the transfer matrix to the path integral for lattice gauge theory, see [42].

Again, we consider a basis describing the field configurations on the lattice at time η such that

$$\hat{U}_{\mathbf{x},\mathbf{e}}^{ab} |U(\eta)\rangle = U_{\mathbf{x},\mathbf{e}}^{ab}(\eta) |U(\eta)\rangle, \quad (\text{G1})$$

We have the initial and final field configurations $|U(0)\rangle$ and $|U(\tau)\rangle$ at time 0 and time τ respectively. The amplitude for one to evolve into the other is

$$\langle U(\tau) | \hat{T}^\tau | U(0) \rangle = \langle U(\tau) | (\hat{W}_{\text{el}} \hat{W}_{\text{mag}})^\tau | U(0) \rangle, \quad (\text{G2})$$

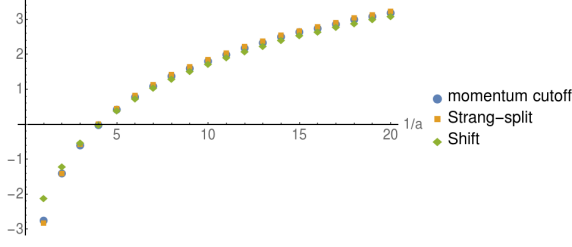


FIG. 8: Here we see the corrections to mass ($\Pi_{\text{Strang}}(p_{\text{in}}^2)$, $\Pi_{\text{cont}}(p_{\text{in}}^2)$ and $\Pi_{\text{shift}}(p_{\text{in}}^2)$) integrated numerically and plotted as a function of the lattice spacing a . Each function has been normalized by subtracting a constant so that they all agree for $a = 2$. We see logarithmic growth with the cutoff in each case with the same prefactor. For the case of a momentum cutoff, we take $\Lambda = \pi/a$. The x axis corresponds to $1/a$, i.e., the inverse lattice spacing, and the y axis is in arbitrary units. In this case, we have taken $\delta t = a/3$ for the Strang-split circuit, and we have taken $p_{\text{in}} = 0$.

where we have

$$\begin{aligned} \hat{W}_{\text{mag}} &= \exp\left(-i\frac{2\kappa}{g^2}\sum_{\mathbf{p}_s}\text{Re}\left(\text{tr}[\hat{U}_{\mathbf{p}_s}]\right)\right) \\ \hat{W}_{\text{el}} &= \prod_{\mathbf{x},\mathbf{e}}\int dV_{\mathbf{x},\mathbf{e}}\exp\left(-i\frac{2}{\kappa g^2}\text{Re}\left(\text{tr}[V_{\mathbf{x},\mathbf{e}}]\right)\right)\hat{L}_{\mathbf{x},\mathbf{e}}(V_{\mathbf{x},\mathbf{e}}). \end{aligned} \quad (\text{G3})$$

Inserting factors of $\mathbb{1} = \int dU(\eta)|U(\eta)\rangle\langle U(\eta)|$, we get

$$\langle U(\tau)|\hat{T}^\tau|U(0)\rangle = \int \prod_1^{\tau-1} dU(\eta) \prod_{\nu=0}^{\tau-1} \langle U(\nu+1)|\hat{T}|U(\nu)\rangle. \quad (\text{G4})$$

Dropping the explicit time dependence, we can simplify this via

$$\langle U'|\hat{W}_{\text{el}}\hat{W}_{\text{mag}}|U\rangle = \langle U'|\hat{W}_{\text{el}}|U\rangle e^{-i\frac{2\kappa}{g^2}\sum_{\mathbf{p}_s}\text{Re}(\text{tr}[U_{\mathbf{p}_s}])}. \quad (\text{G5})$$

Dealing with \hat{W}_{el} is more tricky. First notice that

$$\begin{aligned} \langle U'|\hat{W}_{\text{el}}|U\rangle &= \langle U'|\prod_{\mathbf{x},\mathbf{e}}\int dV_{\mathbf{x},\mathbf{e}}\exp\left(-i\frac{2}{\kappa g^2}\text{Re}\left(\text{tr}[V_{\mathbf{x},\mathbf{e}}]\right)\right)\hat{L}_{\mathbf{x},\mathbf{e}}(V_{\mathbf{x},\mathbf{e}})|U\rangle \\ &= \prod_{\mathbf{x},\mathbf{e}}\exp\left(-i\frac{2}{\kappa g^2}\text{Re}(\text{tr}[U_{\mathbf{x},\mathbf{e}}U_{\mathbf{x},\mathbf{e}}^\dagger])\right). \end{aligned} \quad (\text{G6})$$

At this point, we need to use Gauss' law, which tells us that states are invariant under the transformation $U \rightarrow U^\Omega$, defined by

$$U_{\mathbf{x},\mathbf{e}} \rightarrow \Omega_{\mathbf{x}}U_{\mathbf{x},\mathbf{e}}\Omega_{\mathbf{x}+\mathbf{e}}^\dagger = U_{\mathbf{x},\mathbf{e}}^\Omega \quad (\text{G7})$$

for each \mathbf{x} and \mathbf{e} . Denoting the unitary operator that implements this gauge transformation on states by $D(\Omega)$, we get

$$D(\Omega)|U\rangle = |U^\Omega\rangle = |U\rangle, \quad (\text{G8})$$

where the last equality follows from Gauss' law. Averaging over Ω , we get

$$\begin{aligned} \langle U'|\hat{W}_{\text{el}}|U\rangle &= \int \prod_{\mathbf{y}} d\Omega_{\mathbf{y}} \langle U'|\hat{W}_{\text{el}}D(\Omega)|U\rangle \\ &= \int \prod_{\mathbf{y}} d\Omega_{\mathbf{y}} \prod_{\mathbf{x},\mathbf{e}} \exp\left(-i\frac{2}{\kappa g^2}\text{Re}(\text{tr}[\Omega_{\mathbf{x}}U_{\mathbf{x},\mathbf{e}}\Omega_{\mathbf{x}+\mathbf{e}}^\dagger U_{\mathbf{x},\mathbf{e}}^\dagger])\right). \end{aligned} \quad (\text{G9})$$

If we put back in the time dependence, we can write $U_{\mathbf{x},\mathbf{e}}(\eta) = U_{x,\mathbf{e}}$, where $x = (\eta\delta t, \mathbf{x})$ labels spacetime points. Then, since we are integrating over gauge transformations for each time η , we can just as well rename $\Omega_{\mathbf{x}}(\eta) = U_{x,e^0}$, where e^0 denotes a lattice basis vector in the positive time direction, to get

$$\begin{aligned} \langle U'|\hat{W}_{\text{el}}|U\rangle &= \int \prod_{\mathbf{y}} dU_{y,e^0} \prod_{\mathbf{x},\mathbf{e}} \exp\left(-i\frac{2}{\kappa g^2}\text{Re}(\text{tr}[U_{x,e^0}U_{x,\mathbf{e}}U_{x+\mathbf{e},e^0}^\dagger U_{x,\mathbf{e}}^\dagger])\right). \end{aligned} \quad (\text{G10})$$

But $\text{tr}[U_{x,e^0}U_{x,\mathbf{e}}U_{x+\mathbf{e},e^0}^\dagger U_{x,\mathbf{e}}^\dagger]$ is just the trace of a plaquette unitary, where one of the directions is along the time axis. We can denote all such plaquette unitary by U_{p_t} . Then, denoting spatial plaquettes by p_s , we get

$$\langle U_f|U^\tau|U_i\rangle = \int \mathcal{D}(U)e^{iS(U)}, \quad (\text{G11})$$

where the action $S(U)$ is given by

$$S(U) = \frac{2}{g^2}\left(\frac{a}{\delta t}\sum_{p_t}\text{Re}(\text{tr}[U_{p_t}]) + \frac{\delta t}{a}\sum_{p_s}\text{Re}(\text{tr}[U_{p_s}])\right), \quad (\text{G12})$$

where the sum over spatial plaquettes does not include those at time τ . In the case where $\delta t = a$, this simplifies to become

$$S(U) = \frac{2}{g^2}\sum_p \text{Re}(\text{tr}[U_p]), \quad (\text{G13})$$

where the sum is over all spacetime plaquette unitaries in $\{0, \dots, \tau\} \times \mathbb{Z}^d$ except for spatial plaquettes at time τ . And the measure is given by

$$\mathcal{D}(U) = \prod_{x,e} dU_{x,e}, \quad (\text{G14})$$

where the product includes all spatial links (x, e) with $x^0 \in \{1, \dots, \tau-1\}$ and all temporal links (x, e) with $x^0 \in \{0, \dots, \tau-1\}$. Note that this path integral formalism is mathematically well defined on finite lattices, at least for compact gauge groups.